

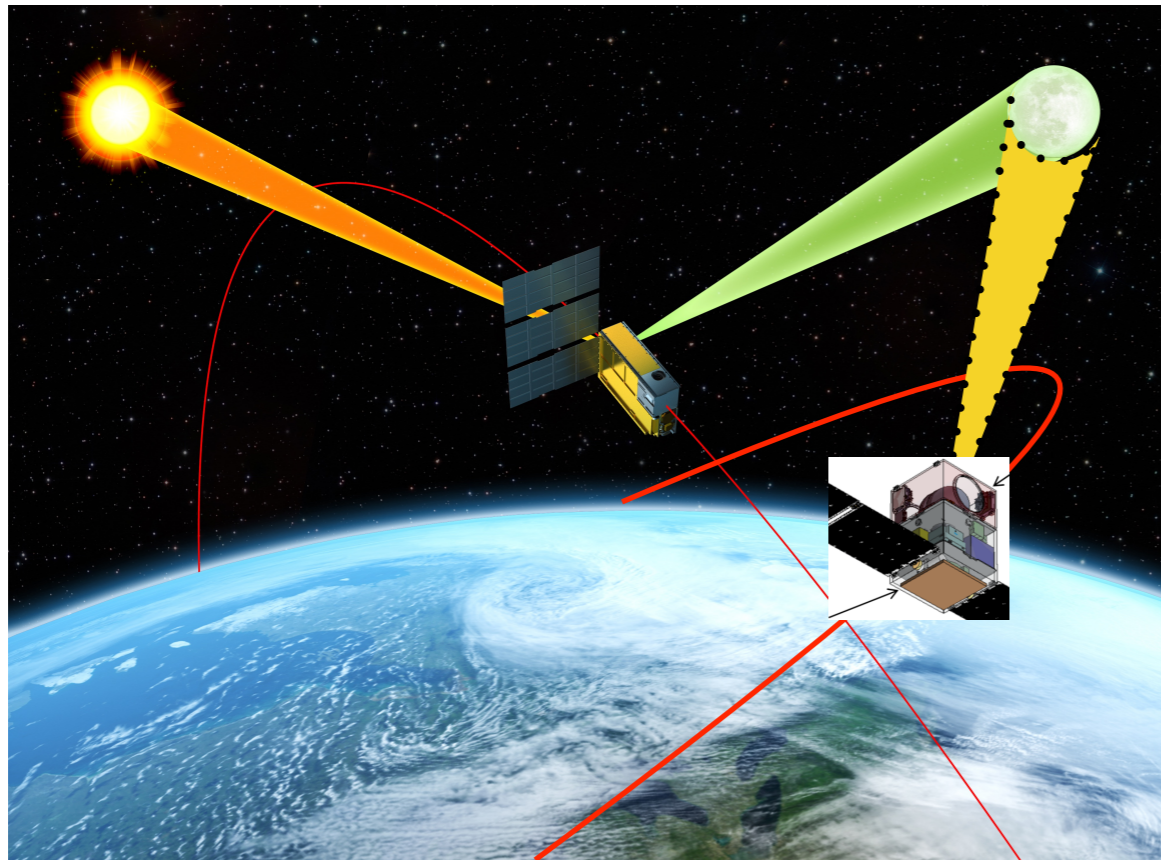
On Developing a SI-Traceable Moon Surface Microwave Emission Model Based on Well Calibrated ATMS/AMSU Observations

Hu(Tiger) Yang
ESSIC, University of Maryland
huyang@umd.edu
Nov.01, 2019

Concept of Lunar Calibration

Advantages of Lunar Calibration

- Accessible for all spacecraft
- Time and location are highly predictable
- Highly stable radiation in microwave band



Lunar Calibration Scheme

Detection of Moon Observations



Calculation of Radiance/
Brightness temperature of Moon



Correction for beam pointing error



Bias evaluation for each
instrument in constellation



Correction for obs. angle and solid
angle of the Moon's Disk



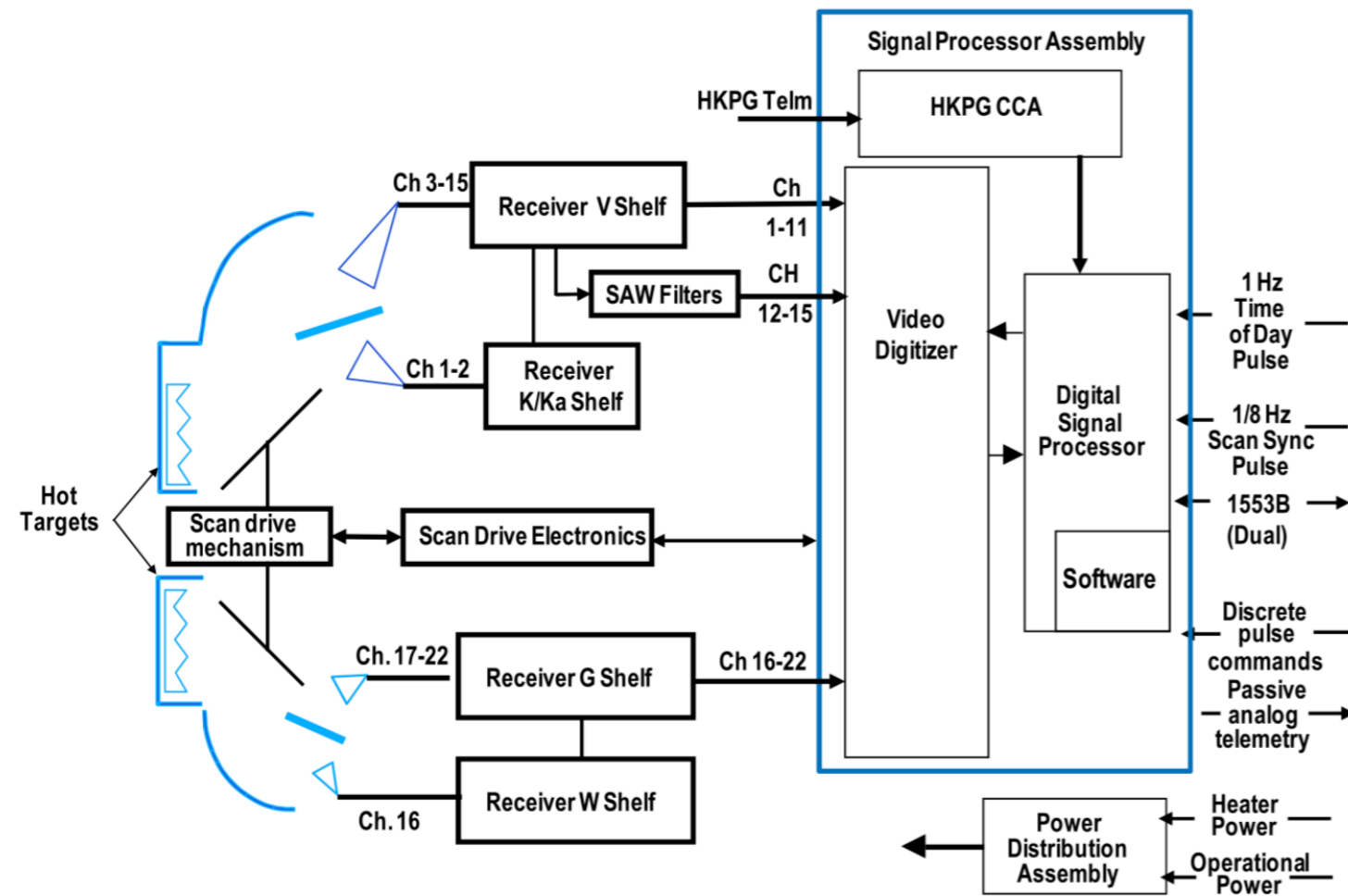
Instrument re-calibration and
inter-satellite calibration

Outline

- Introduction of ATMS instrument
- Physical model for disk integrated microwave emission of Moon
- Microwave brightness temperature spectrum from NOAA-20 ATMS 2-D Moon scan observations
- Phase angle dependent feature derived from drifting orbit of NOAA-18 AMSU
- Conclusion and Future work

ATMS Instrument Description

Simplified ATMS Block Diagram
(Ed Kim et al., JGR 2014)



ATMS Spectrometric and Radiometric Specification

Ch	RF path			Center frequency [MHz]		Bandwidth [MHz]		NEDT [K]	Pol	Beamwidth [°]
	Ant	Feed	Rcvr	Value	Stab	Req	True	Req		
1	A	1	a	23800	<10	<270	1x270	0.5	V	5.2
2	A	1	b	31400	<10	<180	1x180	0.6	V	5.2
3	A	2	c	50300	<10	<180	1x180	0.7	H	2.2
4	A	2	c	51760	<5	<400	1x400	0.5	H	2.2
5	A	2	c	52800	<5	<400	1x400	0.5	H	2.2
6	A	2	c	53596±115	<5	170	2x170	0.5	H	2.2
7	A	2	c	54400	<5	400	1x400	0.5	H	2.2
8	A	2	c	54940	<10	400	1x400	0.5	H	2.2
9	A	2	c	55500	<10	330	1x330	0.5	H	2.2
10	A	2	d ₁	57290.344 [f ₀]	<0.5	330	2x155	0.75	H	2.2
11	A	2	d ₁	f ₀ ±217	<0.5	78	2x 78	1.0	H	2.2
12	A	2	d ₂	f ₀ ±322.2±48	<1.2	36	4x 36	1.0	H	2.2
13	A	2	d ₂	f ₀ ±322.±22	<1.6	16	4x 16	1.5	H	2.2
14	A	2	d ₂	f ₀ ±322.±10	<0.5	8	4x 8	2.2	H	2.2
15	A	2	d ₂	f ₀ ±322.±4.5	<0.5	3	4x 3	3.6	H	2.2
16	B	3	e	88200	<200	2000	1x2000	0.3	V	2.2
17	B	4	f	165500	<200	3000	2x1150	0.6	H	1.1
18	B	4	g	183310±7000	<30	2000	2x2000	0.8	H	1.1
19	B	4	g	183310±4500	<30	2000	2x2000	0.8	H	1.1
20	B	4	g	183310±3000	<30	1000	2x1000	0.8	H	1.1
21	B	4	g	183310±1800	<30	1000	2x1000	0.8	H	1.1
22	B	4	g	183310±1000	<30	500	2x 500	0.9	H	1.1

ATMS Instrument Calibration Error Budget Analysis

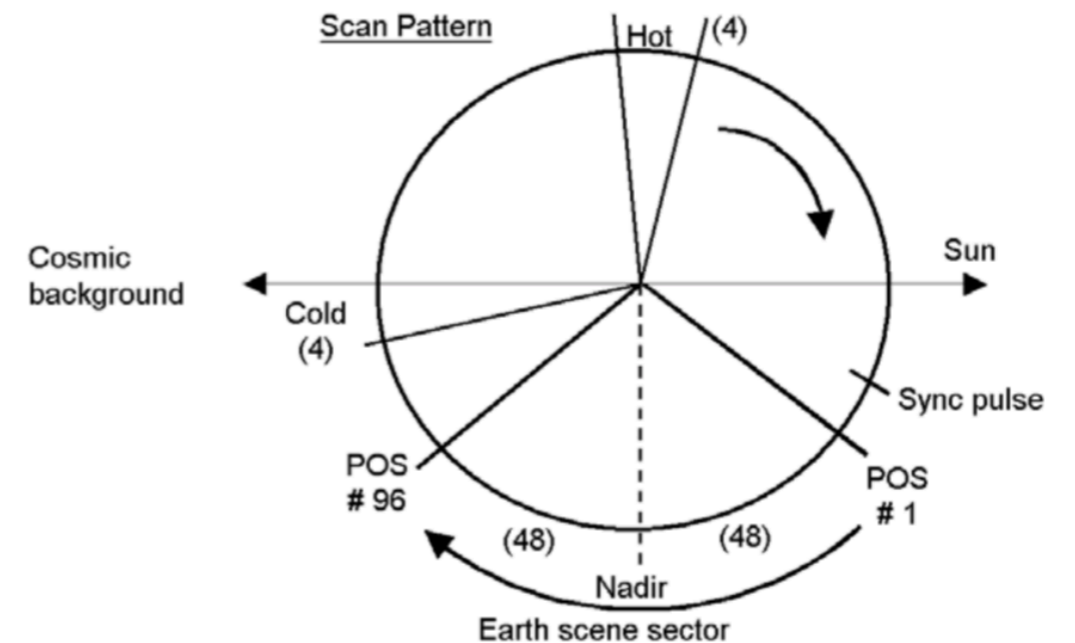
The ATMS radiometric calibration for antenna brightness temperature is derived as

$$R = R_c + (R_w - R_c) \left(\frac{C_s - \overline{C_c}}{C_w - C_c} \right) + Q$$

Considering the system noise and gain drift errors, the error model for ATMS calibration can be derived as:

$$\Delta R = x \Delta R_w + (1 - x) \Delta R_c + 4Q^{\max} (x - x^2) \pm RMSE_{Error}$$

ATMS Scan Geometry



ΔR_w Error in determine warm target radiance

ΔR_c Error in determine cold target radiance

Q^{\max} Maximum nonlinearity

$RMSE_{Error}$ System noise and gain drift errors

Error Budget Results for in-flight SNPP/J1 ATMS

Laboratory microwave calibration standard is needed to make warm load become SI-traceable on-orbit calibration reference

Channel	Warm Target Emissivity	Coupling Loss	Cold-Target Contamination-Earth RMS Error	Peak Non-linearity SNPP ATMS				Peak Non-linearity J1 ATMS			
				RC1	RC2	RC5	RC6	RC1	RC2	RC5	RC6
1	0.999999	0.1205	0.117	0.219	0.278	0.265	0.264	0.59	0.58	0.55	0.55
2	0.999998	0.1205	0.192	0.022	0.093	0.097	0.074	0.64	0.61	0.64	0.63
3	0.999998	0.1154	0.092	0.113	0.172	0.211	0.169	0.01	-0.01	0.00	0.03
4	1.000000	0.1154	0.084	0.212	0.266	0.221	0.239	-0.11	-0.09	-0.11	-0.12
5	1.000000	0.1154	0.092	0.171	0.256	0.242	0.222	-0.06	-0.04	-0.05	-0.07
6	0.999997	0.1154	0.084	0.055	0.117	0.148	0.143	-0.11	-0.09	-0.09	-0.08
7	0.999996	0.1154	0.092	0.061	0.098	0.101	0.093	0.15	0.16	0.15	0.14
8	0.999995	0.1154	0.109	0.164	0.250	0.237	0.222	0.22	0.23	0.24	0.22
9	0.999996	0.1154	0.100	-0.061	0.003	0.020	0.019	0.22	0.21	0.22	0.21
10	0.999997	0.1154	0.084	0.155	0.204	0.156	0.138	0.58	0.60	0.57	0.62
11	0.999997	0.1154	0.084	0.230	0.219	0.282	0.253	0.65	0.59	0.57	0.57
12	0.999997	0.1154	0.084	0.161	0.266	0.214	0.163	0.68	0.76	0.73	0.62
13	0.999997	0.1154	0.084	0.134	0.233	0.215	0.115	0.79	0.80	0.77	0.76
14	0.999997	0.1154	0.084	-0.130	-0.113	-0.062	0.010	0.56	0.69	0.54	0.68
15	0.999997	0.1154	0.084	0.192	0.292	0.098	0.219	0.59	0.72	0.68	0.56
16	0.999999	0.0760	0.326	0.240	0.296	0.309	0.327	0.16	0.17	0.15	0.12
17	0.999983	0.0551	0.050	0.304	0.390	0.384	0.397	0.46	0.44	0.41	0.42
18	0.999964	0.0551	0.067	0.227	0.289	0.277	0.308	0.20	0.20	0.21	0.19
19	0.999964	0.0551	0.067	0.270	0.308	0.350	0.351	0.18	0.17	0.18	0.18
20	0.999964	0.0551	0.067	0.324	0.302	0.338	0.337	0.15	0.18	0.19	0.16
21	0.999964	0.0551	0.067	0.246	0.282	0.287	0.357	0.14	0.20	0.24	0.14
22	0.999979	0.0551	0.025	0.305	0.295	0.349	0.343	0.38	0.34	0.31	0.35

Peer Review Publications for ATMS Cal/Val Sciences

Calibration Algorithm

- Edward Kim Cheng-Hsuan J. Lyu Kent Anderson R. Vincent Leslie William J. Blackwell, 2014, “S-NPP ATMS instrument prelaunch and on-orbit performance evaluation” JGR, 2014 <https://doi.org/10.1002/2013JD020483>
- Fuzhong Weng, Xiaolei Zou, Ninghai Sun, Hu Yang, Xiang Wang, Lin Lin, Miao Tian, and Kent Anderson, 2013, “Calibration of Suomi National Polar-Orbiting Partnership (NPP) Advanced Technology Microwave Sounder (ATMS)”, Journal of Geophysical Research, Vol.118, No.19, PP. 11,187~11,200
- Weng, F. and Yang, H., 2016. Validation of ATMS calibration accuracy using Suomi NPP pitch maneuver observations. Remote Sensing, 8(4), p.332

Antenna Correction

- Hu Yang and Fuzhong Weng, Kent Anderson, 2016, "Estimation of ATMS Antenna Emission from Cold Space Observations", , IEEE Geoscience and Remote sensing, 10.1109/TGRS.2016.2542526”
- Fuzhong Weng, Hu Yang, Xiaolei Zou, 2013, “On Convertibility From Antenna to Sensor Brightness Temperature for ATMS”, IEEE Geoscience and Remote sensing Letters, 2012, Vol.99, pp 1-5

Remapping SDR

- Hu Yang and Xiaolei Zou, X, 2014. Optimal ATMS remapping algorithm for climate research. Geoscience and Remote Sensing, IEEE Transactions on Geoscience and Remote Sensing, 52(11), 7290-7296.

Lunar Contamination Correction

- Hu Yang and Fuzhong Weng, 2016, “On-Orbit ATMS Lunar Contamination Corrections”, IEEE Transactions on Geoscience and Remote Sensing, Vol. 54 Issue: 4, page(s): 1-7

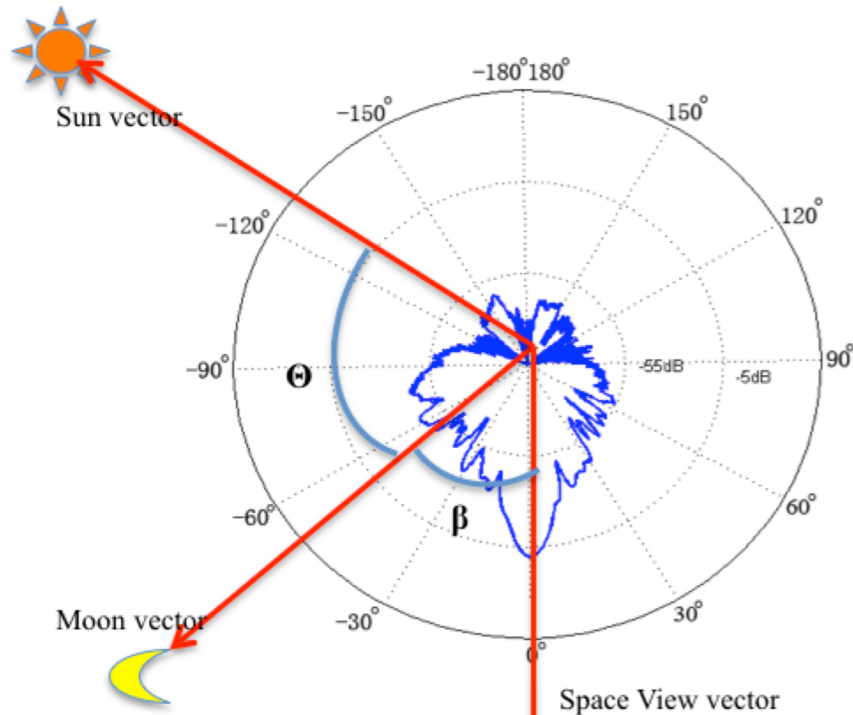
Vicarious calibration and Long-term stability Monitoring

- Hu Yang, Jun Zhou, Ninghai Sun, Kent Anderson, Quanhua Liu, Ed Kim, 2018, “Developing vicarious calibration for microwave sounding instruments using lunar radiation”, IEEE Transactions on Geoscience and Remote Sensing, Vol.99, PP.1-11

Geolocation correction and Validation

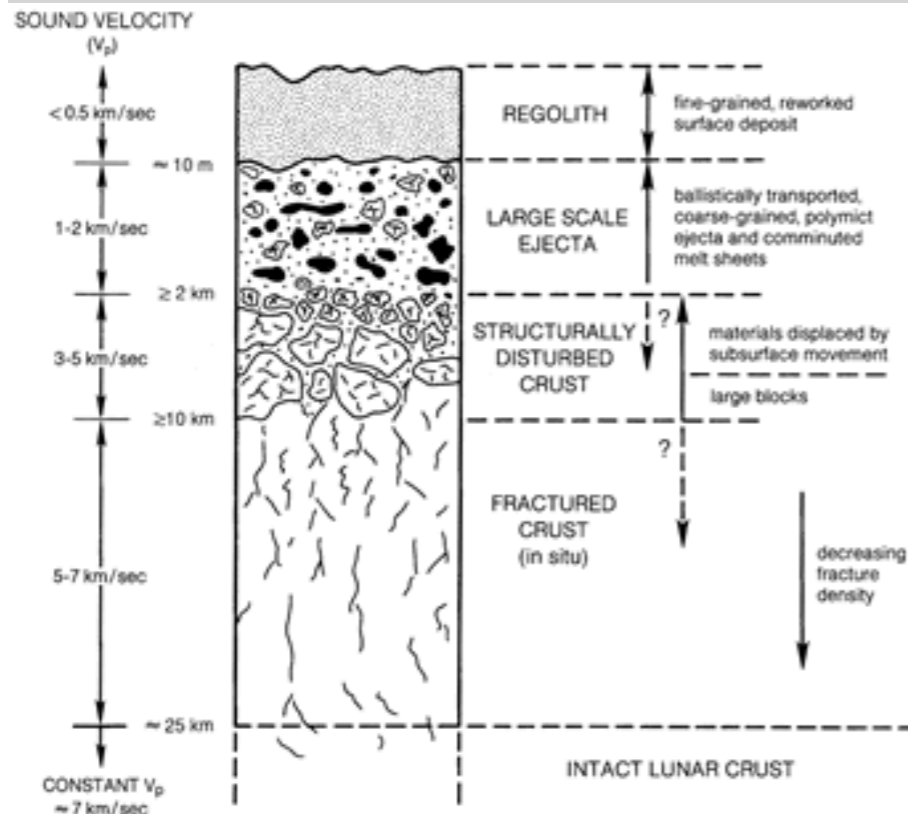
- Jun Zhou and Hu Yang, 2019, “On Study of Two-Dimensional Lunar Scan for Advanced Technology Microwave Sounder Geometric Calibration”, Atmospheric Measurement Technique, <https://doi.org/10.5194/amt-2019-177>
- Jun Zhou, Hu Yang and Kent Anderson, 2019, “SNPP ATMS On-Orbit Geolocation Error Evaluation and Correction Algorithm”, IEEE Transactions on Geoscience and Remote Sensing 57 (6), 3802-3812

Physical Model for Antenna Temperature of the Moon's Disk



Lunar Surface Structure

Heiken, G.H., Vaniman, D.T., & French, B.M. eds, **Lunar Sourcebook**, Lunar and Planetary Institute, Houston, 1991.



When the Moon appears in satellite observation field of view (FOV), the effective microwave brightness temperature of moon's disk, can be expressed as function of antenna response function G_{ant} , normalized solid angle of the moon Ω_{moon} , and average brightness temperature of the moon's disk :

$$TB_{moon}^{eff} = \Omega_{moon} \cdot G_{ant} \cdot TB_{moon}^{disk}$$

Assuming the azimuthal asymmetry is insignificant, the antenna response within the mean beam range can then be accurately simulated by one dimension Gaussian function:

$$G_{ant}(\beta') = e^{-\frac{(\beta' - \alpha_0)^2}{2 \cdot \sigma^2}}$$

where β is the separation angle between antenna boresight and Moon-in-View vector, α_0 is the beam pointing error angle. The normalized solid angle of moon is calculated as a solid angle of moon disk normalized by the beam solid angle, :

$$\Omega_{moon} = \frac{\pi \left(\frac{r_{moon}}{D_{moon}} \right)^2}{\Omega_A}$$

Beam solid angle can be calculated from ground measured antenna pattern data as:

$$\Omega_A = \iint_{4\pi} G(\theta, \phi) \sin\theta \, d\theta \, d\phi$$

Theoretical Modeling Approach for Microwave Emission of the Moon's Disk

RADIO EMISSION AND NATURE OF THE MOON

V. D. KROTIKOV and V. S. TROITSKIĬ

Usp. Fiz. Nauk 81, 589-639 (December, 1963)

$$\bar{T}_e = (1 - R_{\perp}) \beta_0 T_0(0) + (1 - R_{\perp}) \sum_{n=1}^4 (-1)^{\alpha_n} \frac{T_n(0) \beta_n}{\sqrt{1 + 2\delta_n + 2\delta_n^2}} \times \cos(n\Phi - \varphi_n - \xi_n - \Delta\xi_n), \quad (17)$$

where

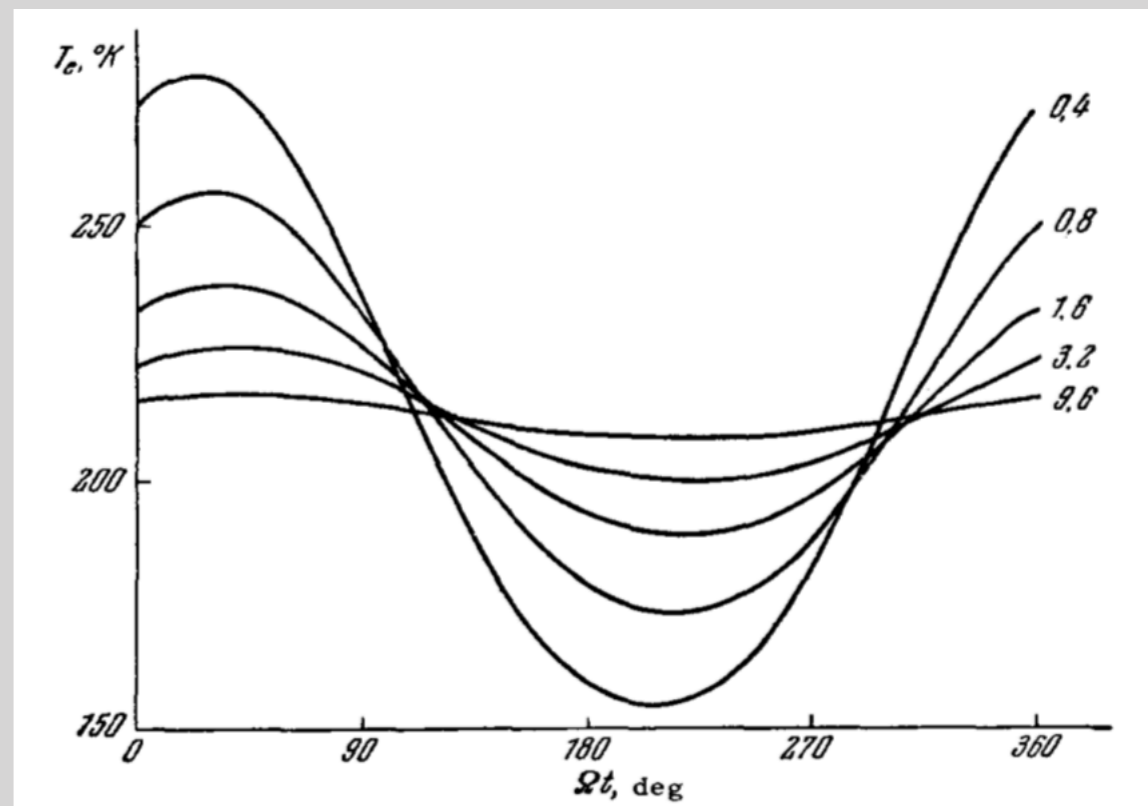
$$(1 - R_{\perp}) \beta_0 T_0(0) = \bar{T}_{e0}$$

is the constant component of the effective temperature averaged over the coordinates*,

$$\frac{T_n(0) \beta_n}{\sqrt{1 + 2\delta_n + 2\delta_n^2}}$$

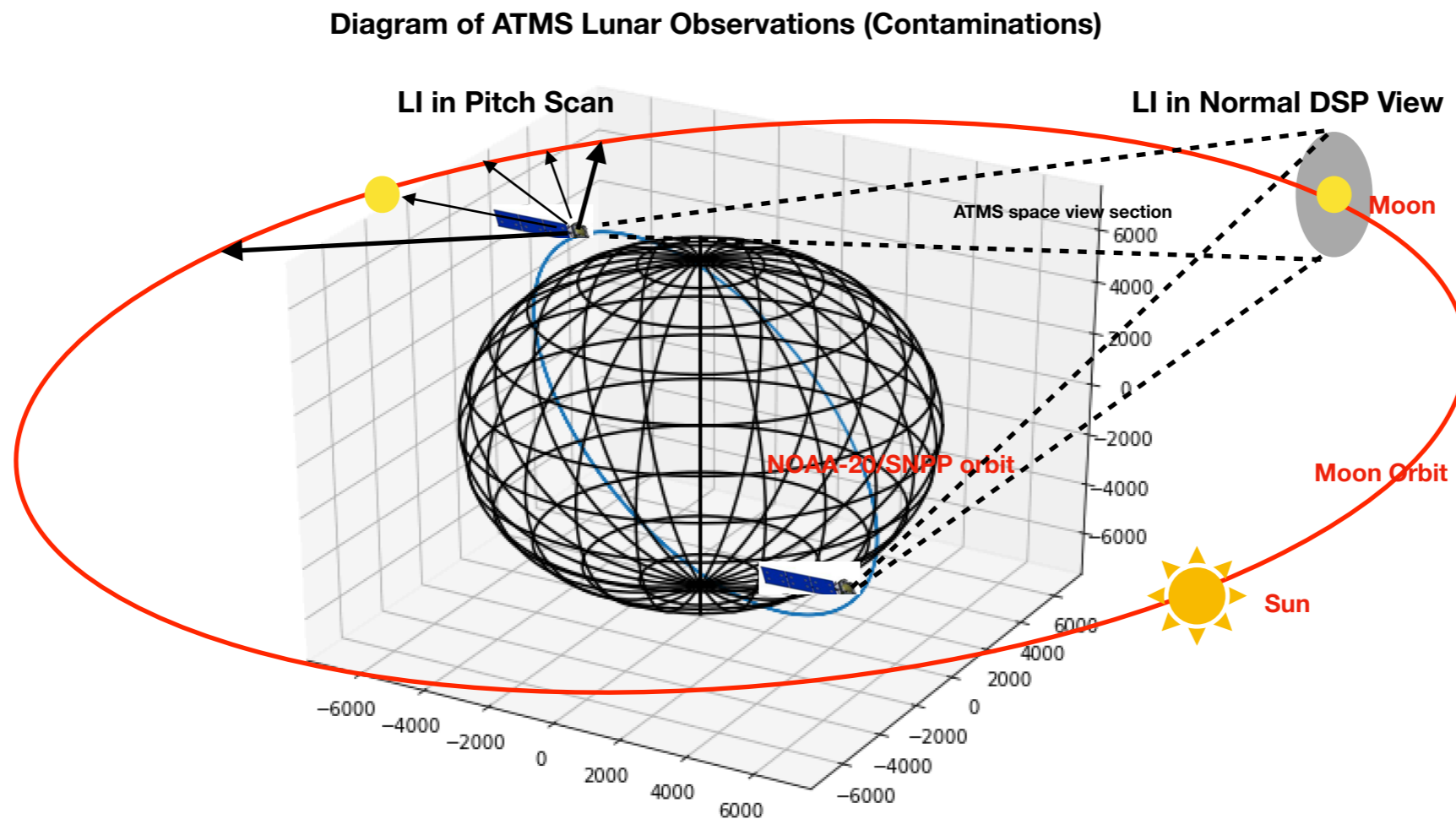
is the n-th harmonic of the effective temperature averaged over the disc, β_0 and β_n are the corresponding averaging coefficients, and $\Delta\xi_n$ is the additional phase shift resulting from the averaging.

Model Simulations of T_e Averaged over the Moons Disk at Different Wavelength

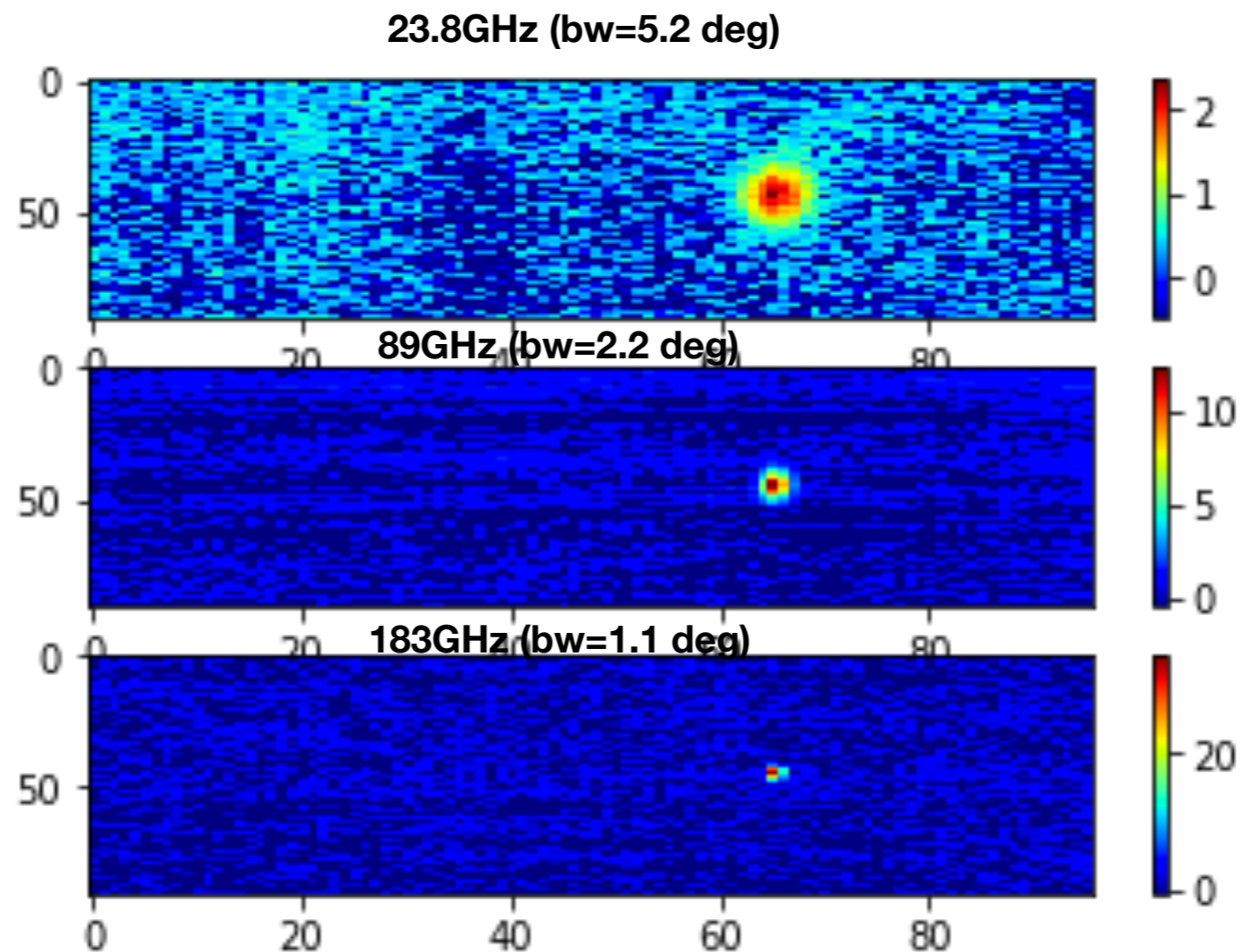


Two-Dimension Lunar Scan Observations from NOAA020 ATMS

The NOAA-20 satellite was successfully launched on 18 November 2017. On January 31, 2018, the spacecraft performed a pitch-over maneuver operation, during which the two-dimensional lunar scan observations were collected. Due to the orientation of NOAA-20 orbits, radiation from a full Moon disk with closely to 180 deg phase angle were collected when the Moon passing through the antenna beam

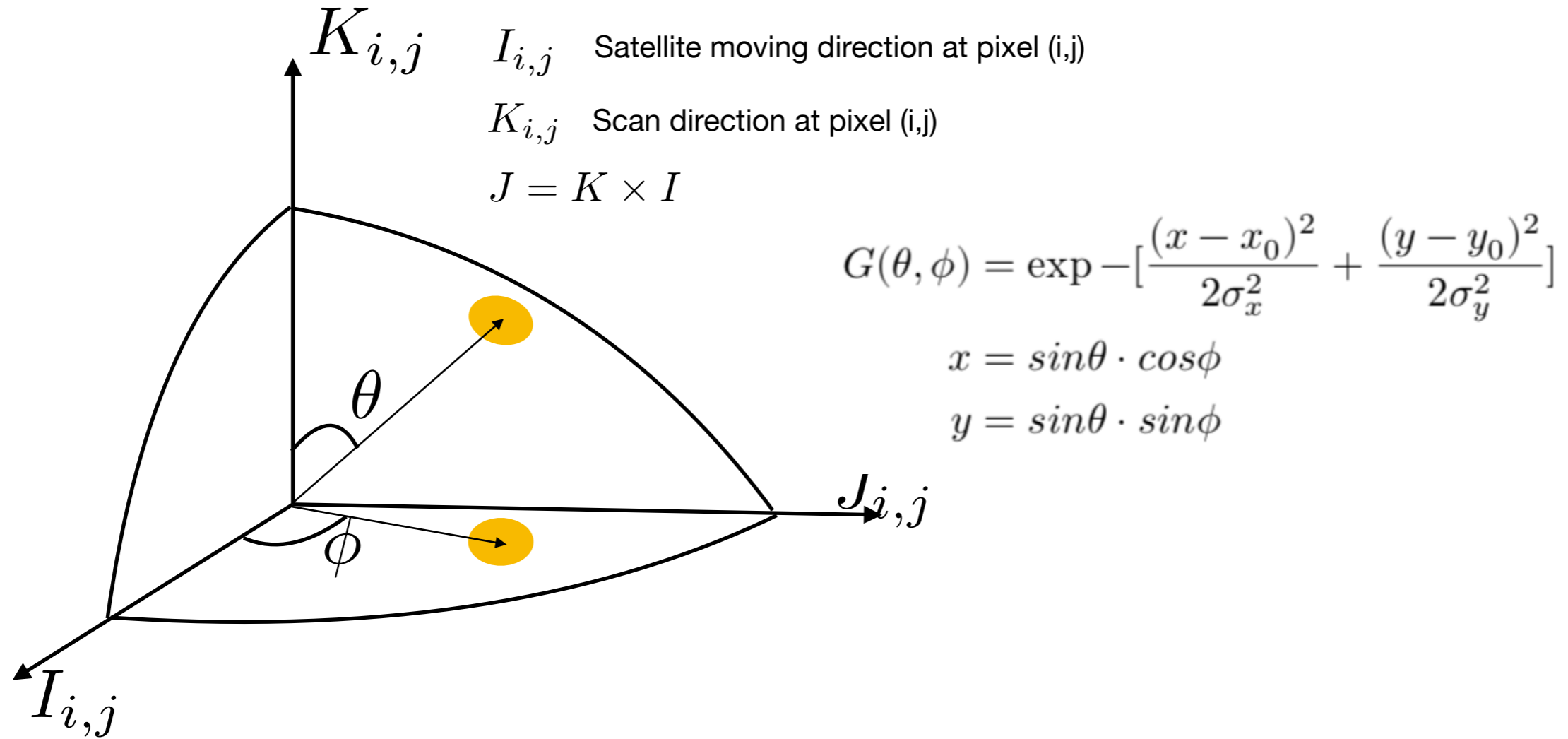


- The observed raw data counts were transferred to brightness temperature by using the calibration equation with the warm load and cold space observations.
- Further corrections for warm bias, earth side lobe contamination, as well as the reflector emission contamination are needed.
- To derive the pure lunar signal, the cosmic background radiation is subtracted from the calibrated brightness temperature.



2-D Physical Model for Microwave Moon Observations

Dynamic Antenna Coordinate System for Lunar Scan



$$T_{a_{moon}}(\theta_{ifov}, \phi_{ifov}) = \frac{T_{b_{moon}}^{Disk} \Omega_{moon}}{\Omega_p} G(\theta_{ifov}, \phi_{ifov})$$

$T_{a_{moon}}(\theta_{ifov}, \phi_{ifov})$ observed antenna temperature of Moon

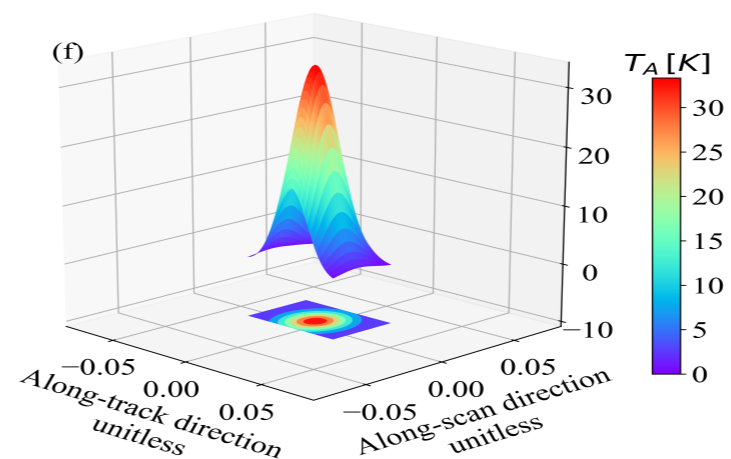
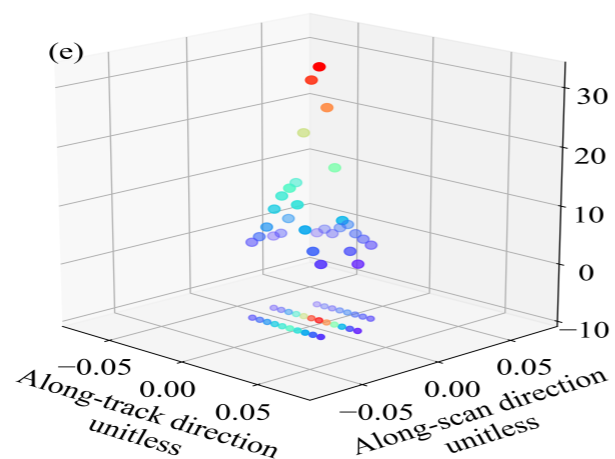
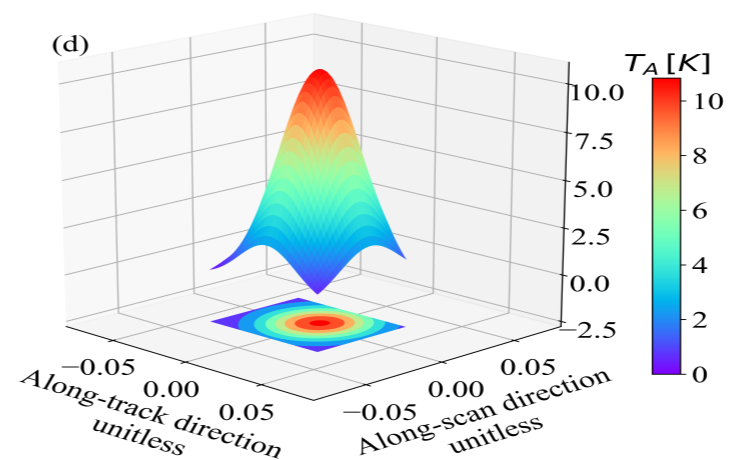
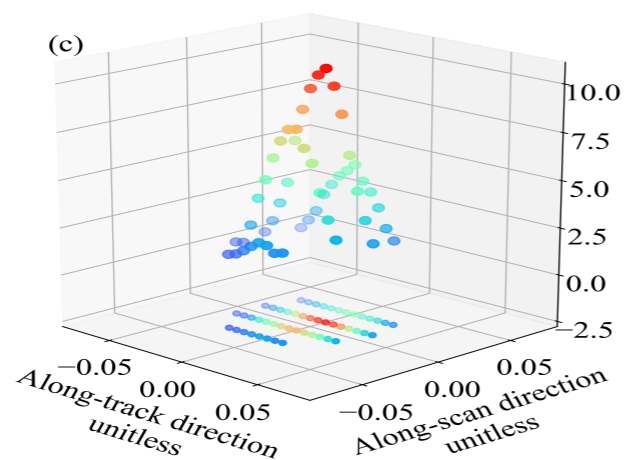
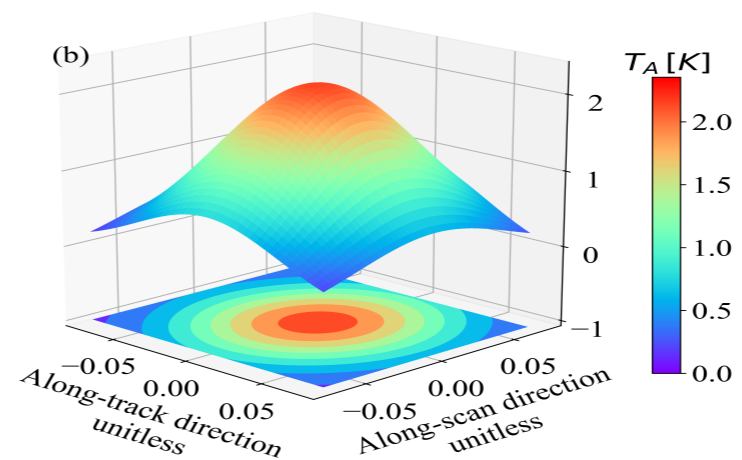
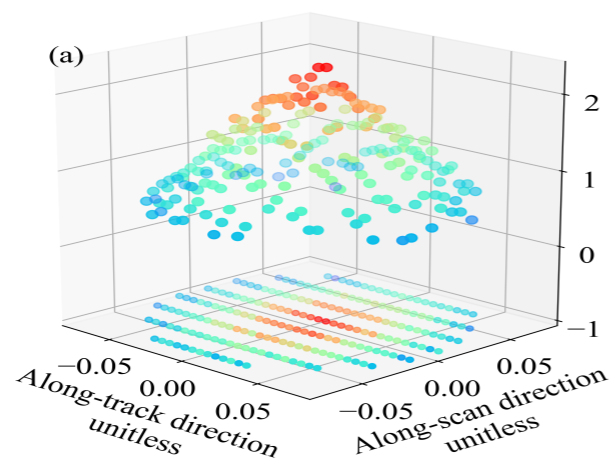
$T_{b_{moon}}^{Disk}$ Disk integrated brightness temperature of lunar surface

Ω_{moon} Solid angle of Moon at observed antenna beam width

Ω_p Antenna solid angle

$G(\theta_{ifov}, \phi_{ifov})$ Antenna response of lunar observations at specified scan position

2D Gaussian Interpolation over the Original Observations

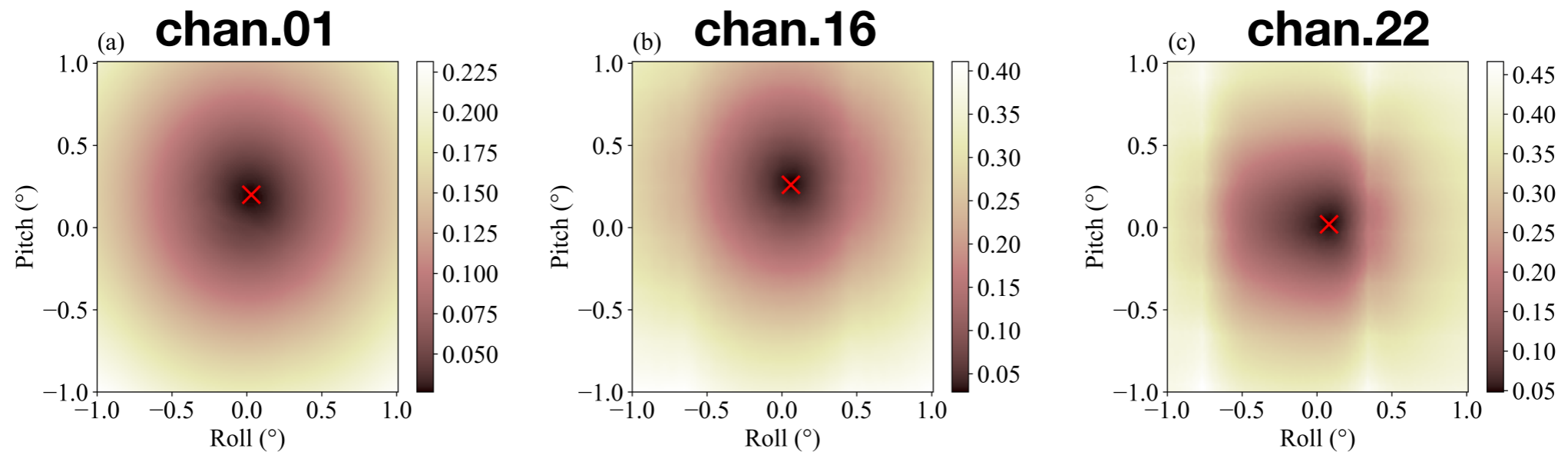


Beam Pointing Error Assessment

Considering the facts that the magnitude of antenna response is very sensitive to position of Moon's center in the Field of View of antenna beam on observing direction. Especially when lunar appears at the center of FOV, where the gradient of antenna response reaches its maximum. Therefore by comparing simulated antenna response of lunar scans with the observation truth, the displacement of beam center can be identified.

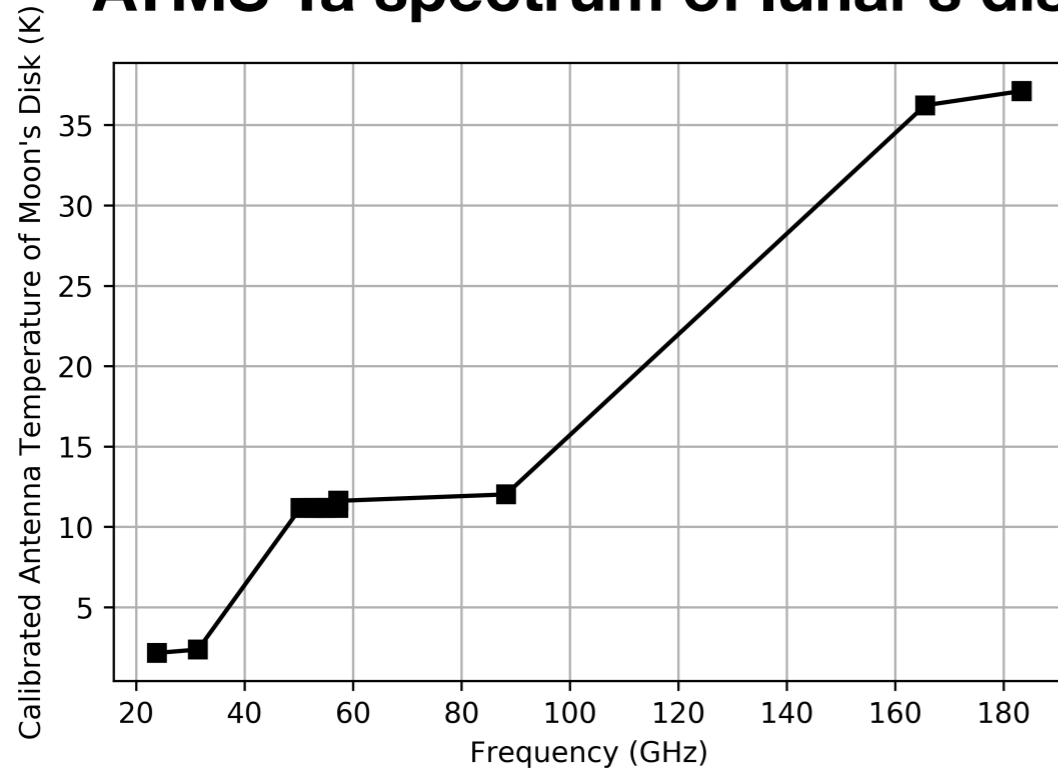
Given (ξ_r, ξ_p) are roll and pitch Euler angles error in ATMS geometric calibration, the optimum (ξ_r, ξ_p) value can be determined by finding the minima of the function below:

$$\sigma(\xi_r, \xi_p) = \frac{1}{N-1} \sqrt{\sum_{i=1}^N (G(\xi_r, \xi_p) - G_{obs})^2}$$



Retrieving of Lunar Microwave Brightness Temperature Spectrum

ATMS Ta spectrum of lunar's disk

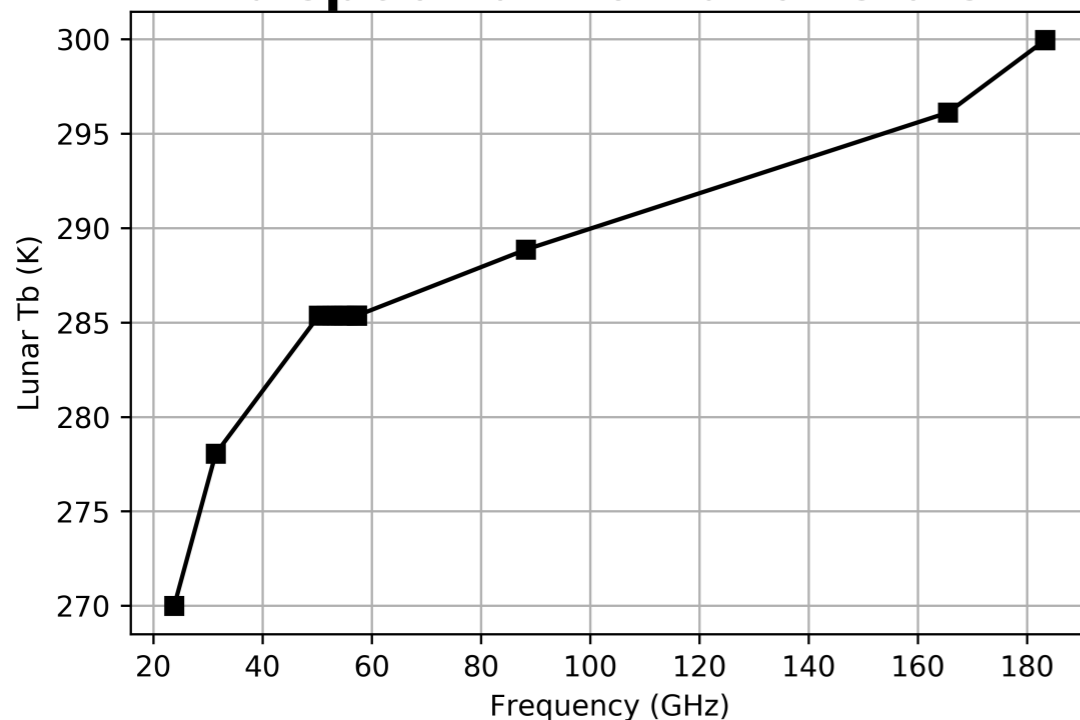


original lunar observations were calibrated to radiance, with instrument nonlinearity, cold background radiation, as well as the thermal emission from antenna reflector were corrected and removed from observations

$$R = R_c + (R_w - R_c) \left(\frac{C_s - \overline{C_c}}{C_w - \overline{C_c}} \right) + Q$$

$$R^{moon} = R - R_c - Sa$$

Tb spectrum of lunar's disk



By combined using ground measured antenna parameters and on-orbit derived antenna responses of lunar radiation, the disk-integrated lunar microwave brightness temperature spectrum can then be derived from well-calibrated lunar antenna temperature

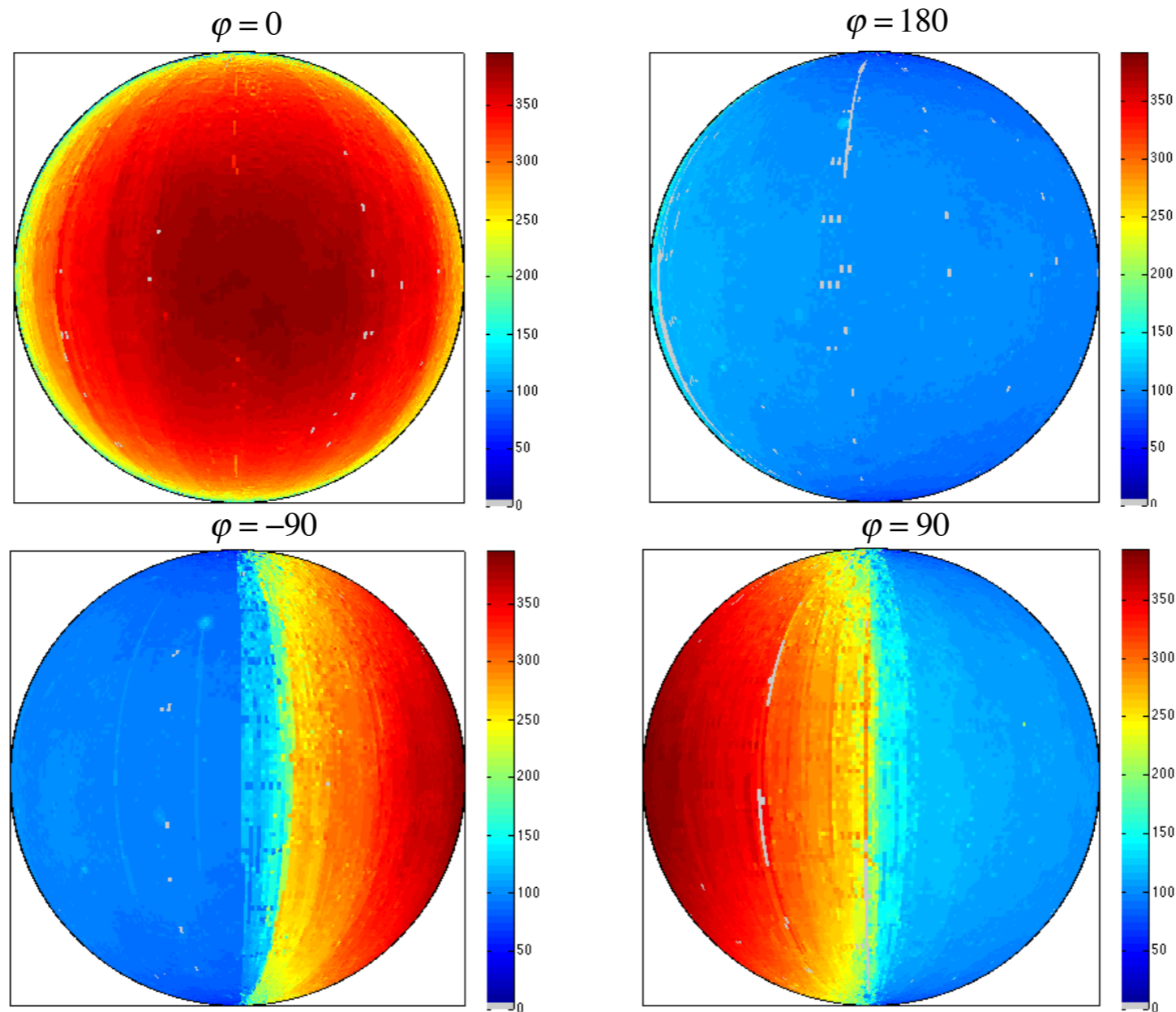
$$T_{a_{moon}}(\theta_{ifov}, \phi_{ifov}) = \frac{T_{b_{moon}}^{Disk} \cdot \Omega_{moon}^{max}}{\Omega_p} G(\theta_{ifov}, \phi_{ifov})$$

$$T_{a_{moon}} = T_{a_{moon}}^{max} \cdot G(\theta, \phi)$$

$$T_{b_{moon}}^{Disk} = \frac{\Omega_p \cdot T_{a_{moon}}^{max}}{\Omega_{moon}^{max}}$$

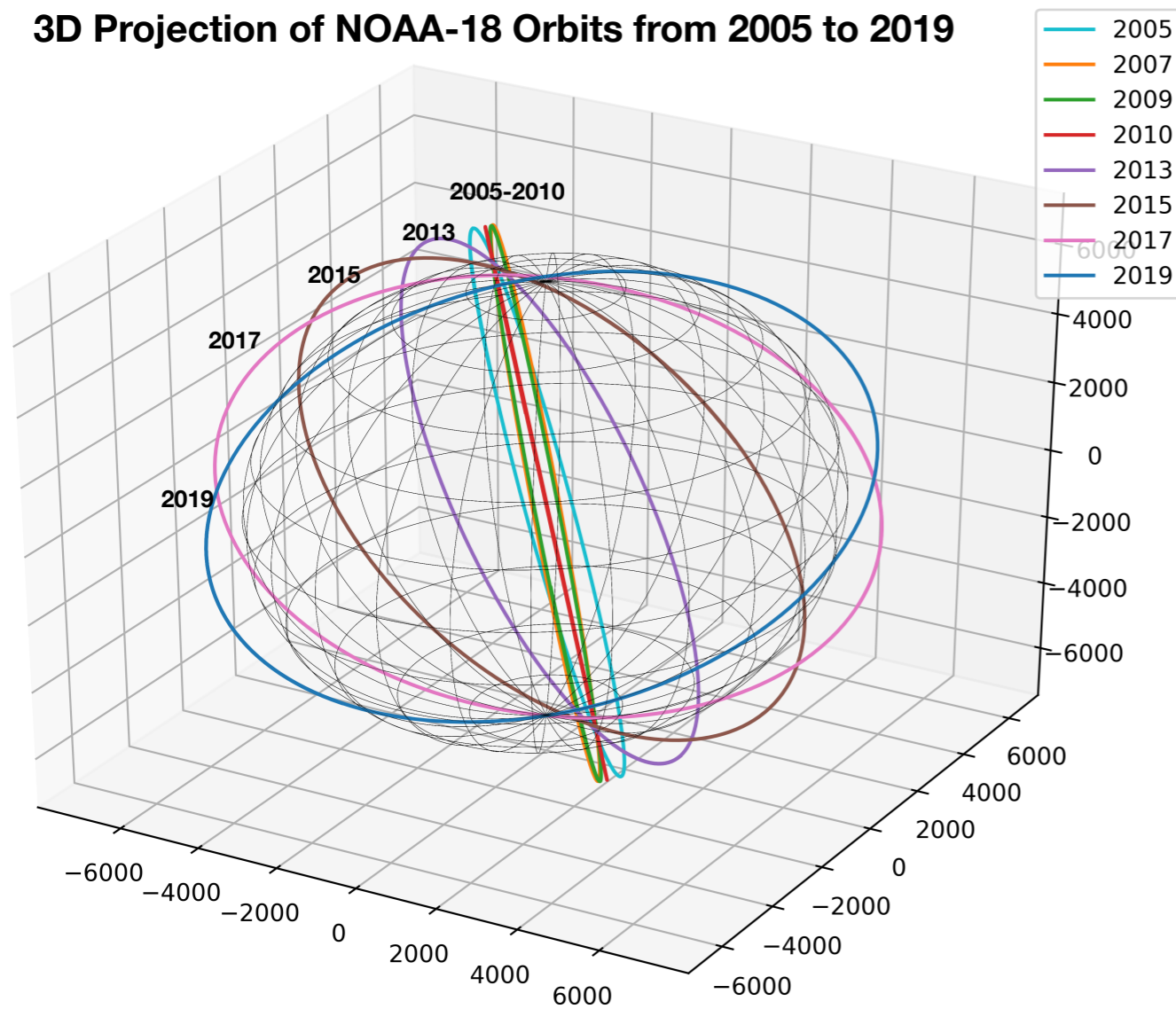
Moon Phase Angle Dependent Feature in Microwave Brightness Temperature of Moon's Surface

Moon surface temperature derived from the Diviner Lunar Radiometer
Experiment instrument (DLRE) observations

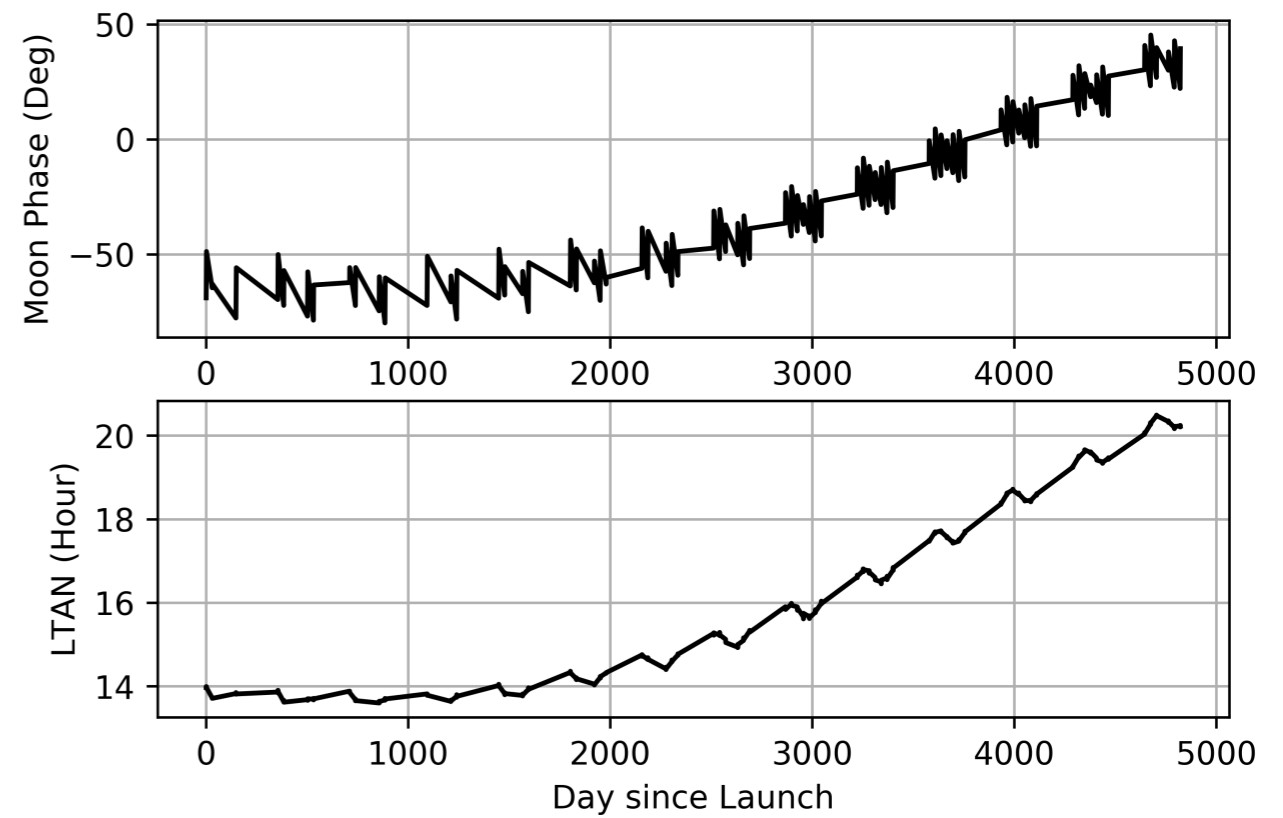


Moon Observations from AMSU Instrument on Drifting NOAA-18 Satellite

3D Projection of NOAA-18 Orbits from 2005 to 2019



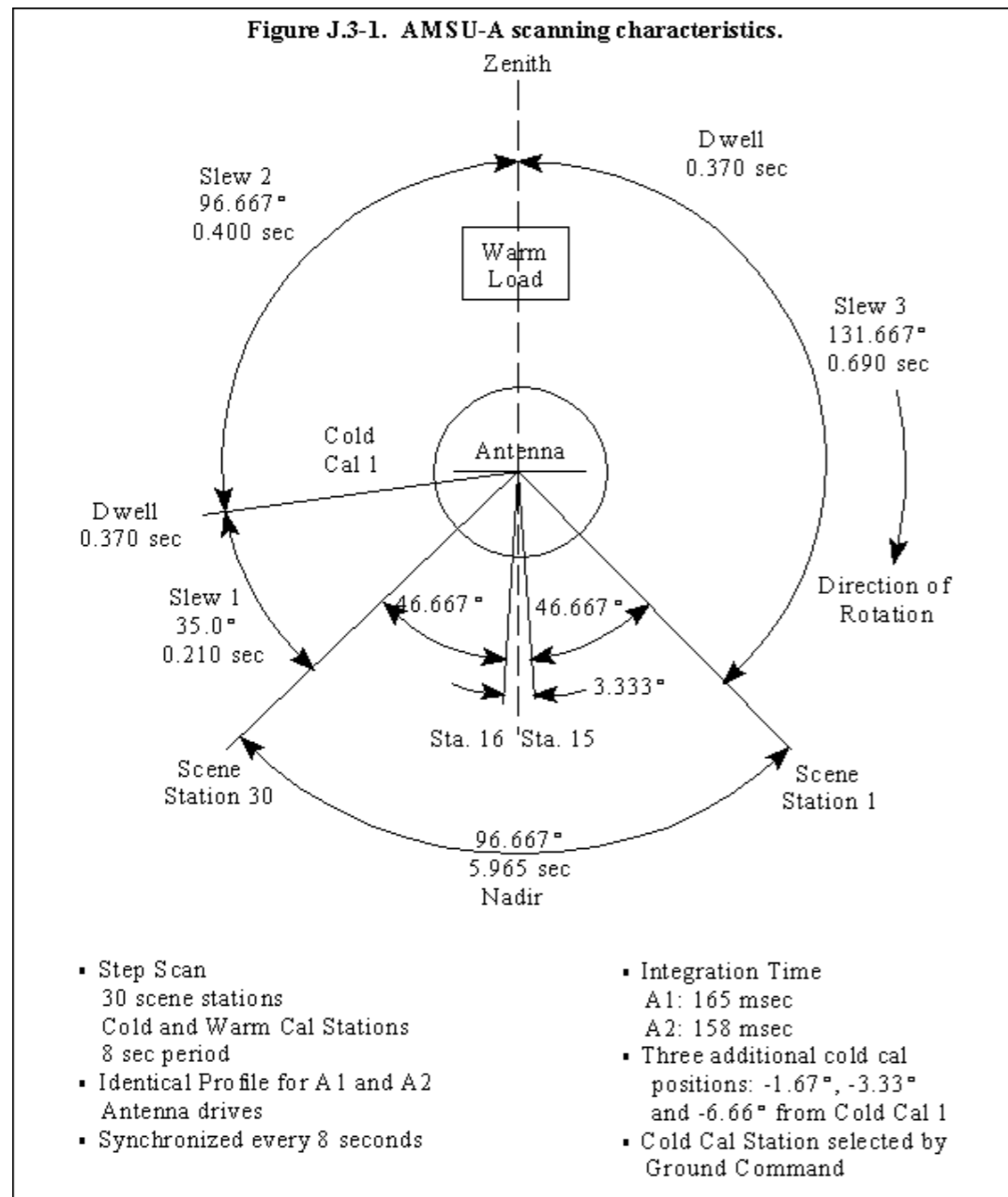
Change of Moon Phase Angle and LTAN of NOAA-18 Satellite



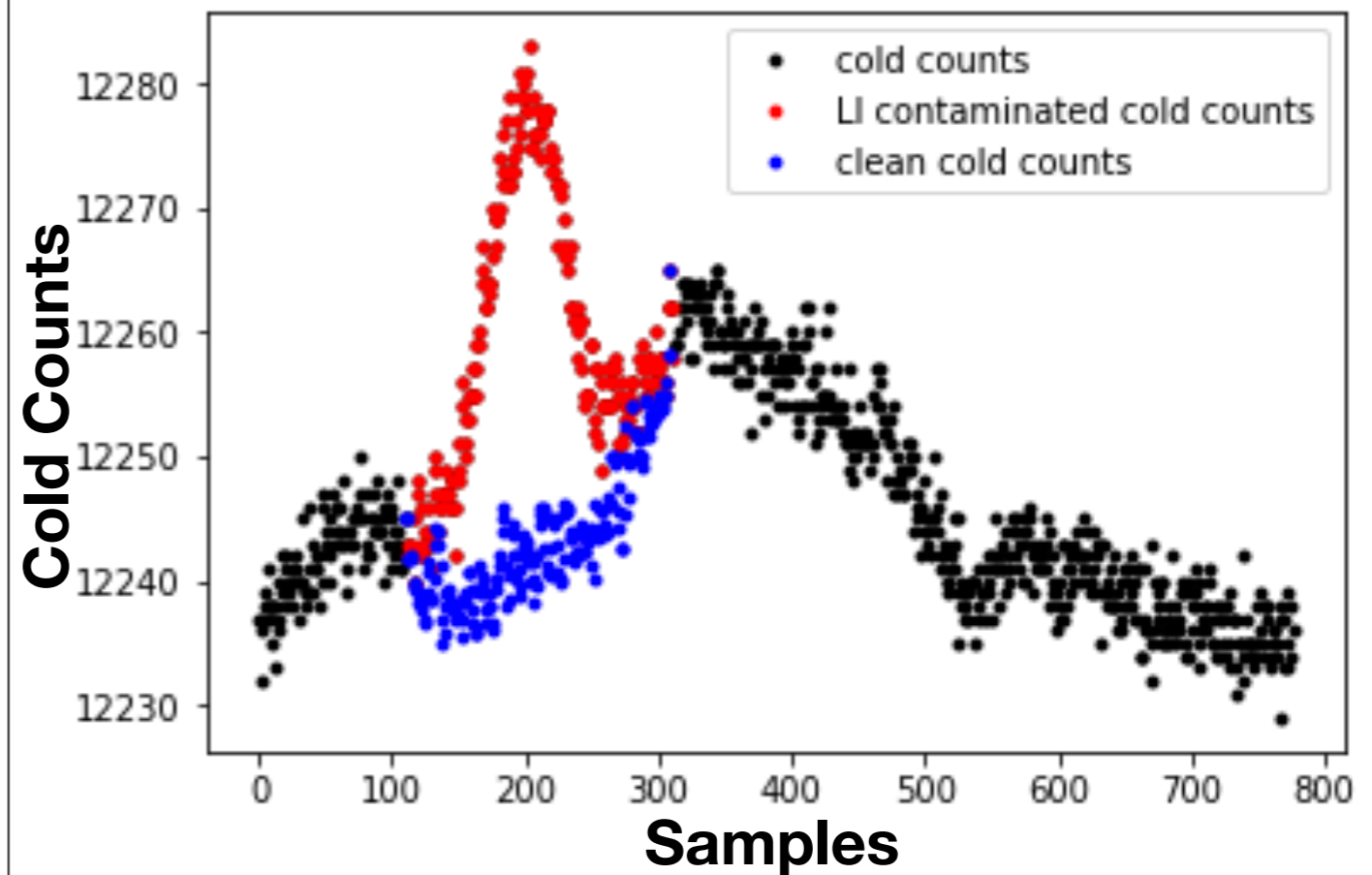
AMSU Lunar Intrusion Data Sampling and Calibration

- AMSU LI samples can be identified from the position of Moon at the rotation antenna coordinate system.
- There is only one space view sample available at each scan of AMSU instrument, the searching for “clean” reference calibration counts is challenging since the calibration gain is keep changing during the LI process.
- LI free “clean” space view closest to the LI samples was taken to be reference at the starting time, then a successive substitution method was applied to derive the reference calibration counts

AMSU Scan Geometry



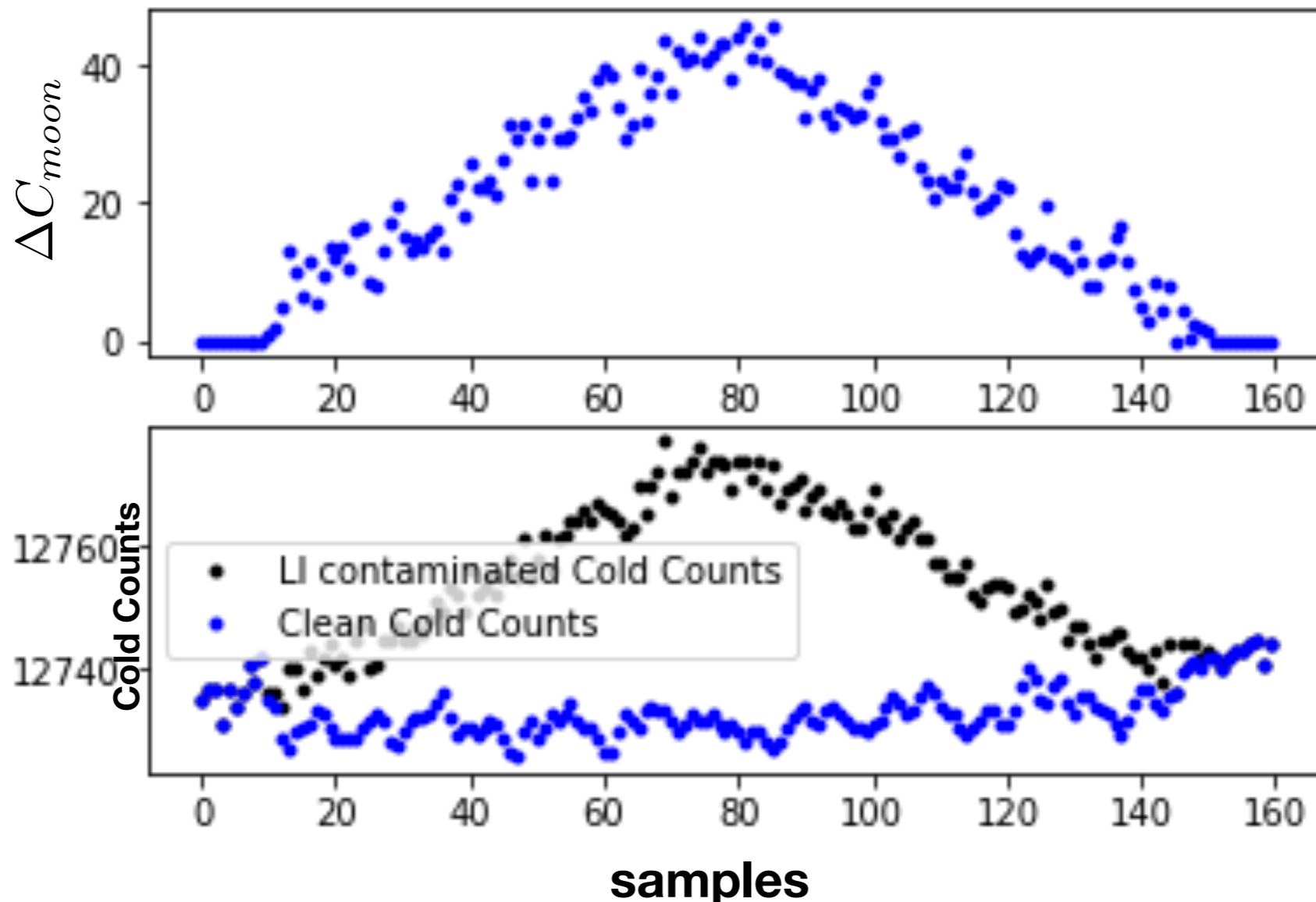
AMSU Channel 01 LI Samples



Calibration of lunar antenna temperature and Moon's disk integrated brightness temperature

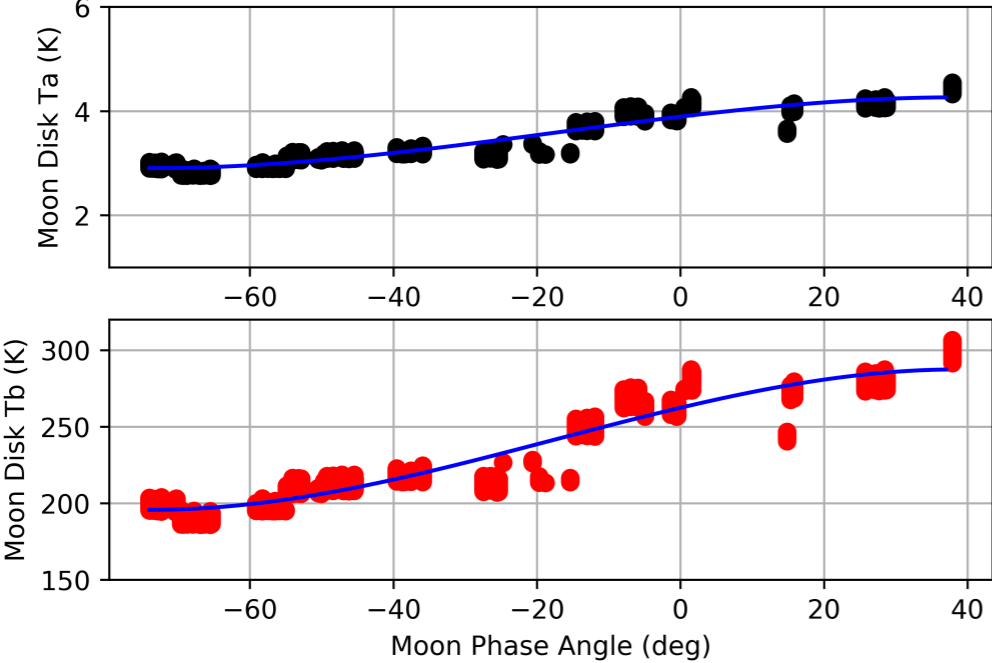
Considering the fact that antenna pattern kept unchanged over the time, Moon brightness temperature spectrum at full moon phase from ATMS are used as anchor to derive AMSU antenna parameters. T_b at all other Moon phase angle can then be derived from the corrected antenna temperature

$$T_{a_{moon}} = G \cdot \Delta C_{moon} \quad T_{b_{moon}} = \frac{T_{a_{moon}}}{\Omega_{moon}}$$

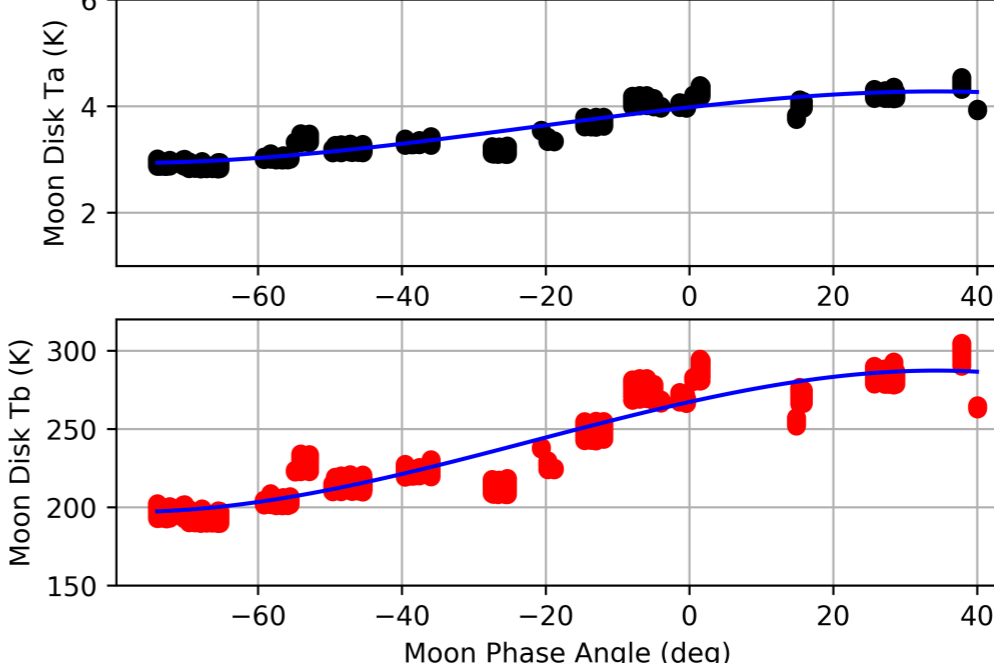


Moon Phase Angle Dependent Feature in Different Microwave Frequencies

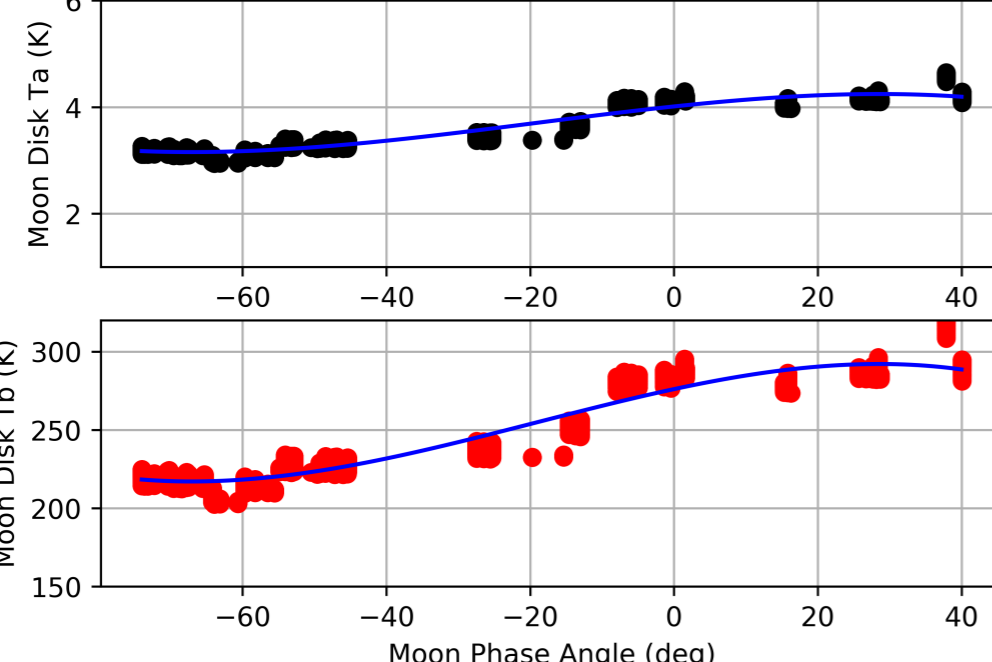
23 GHz



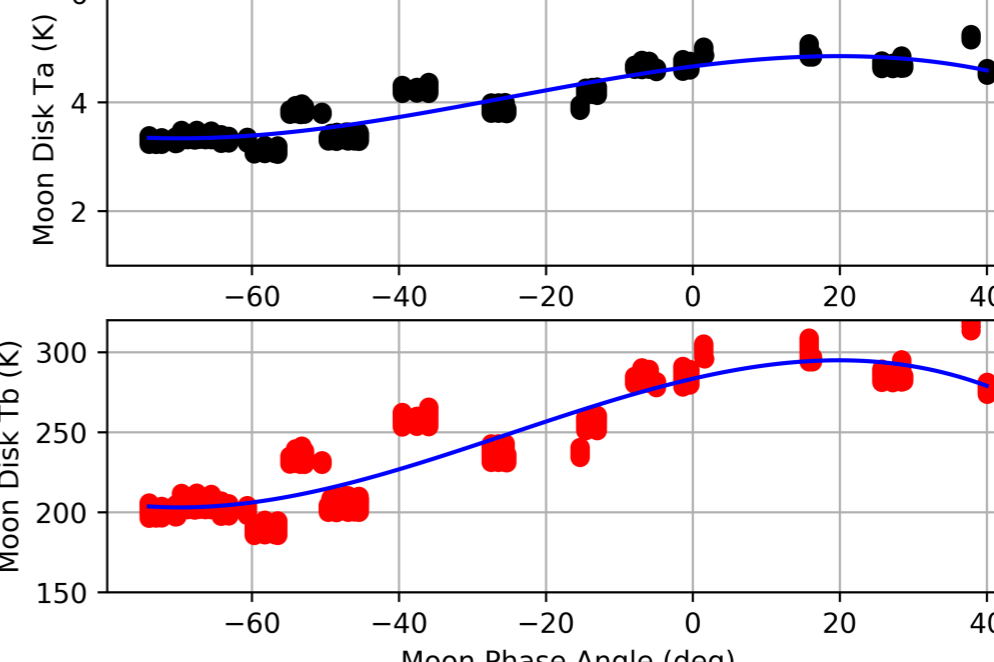
34GHz



57GHz



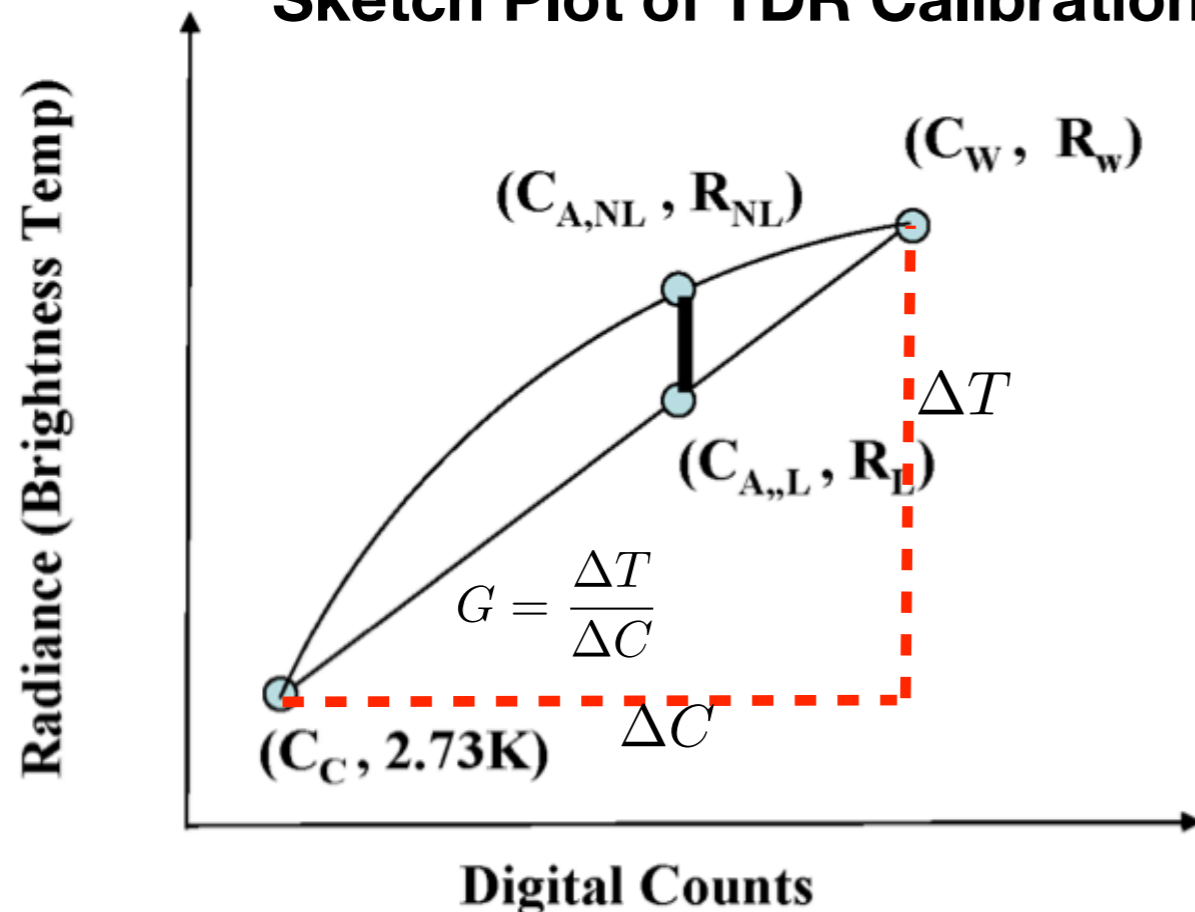
89GHz



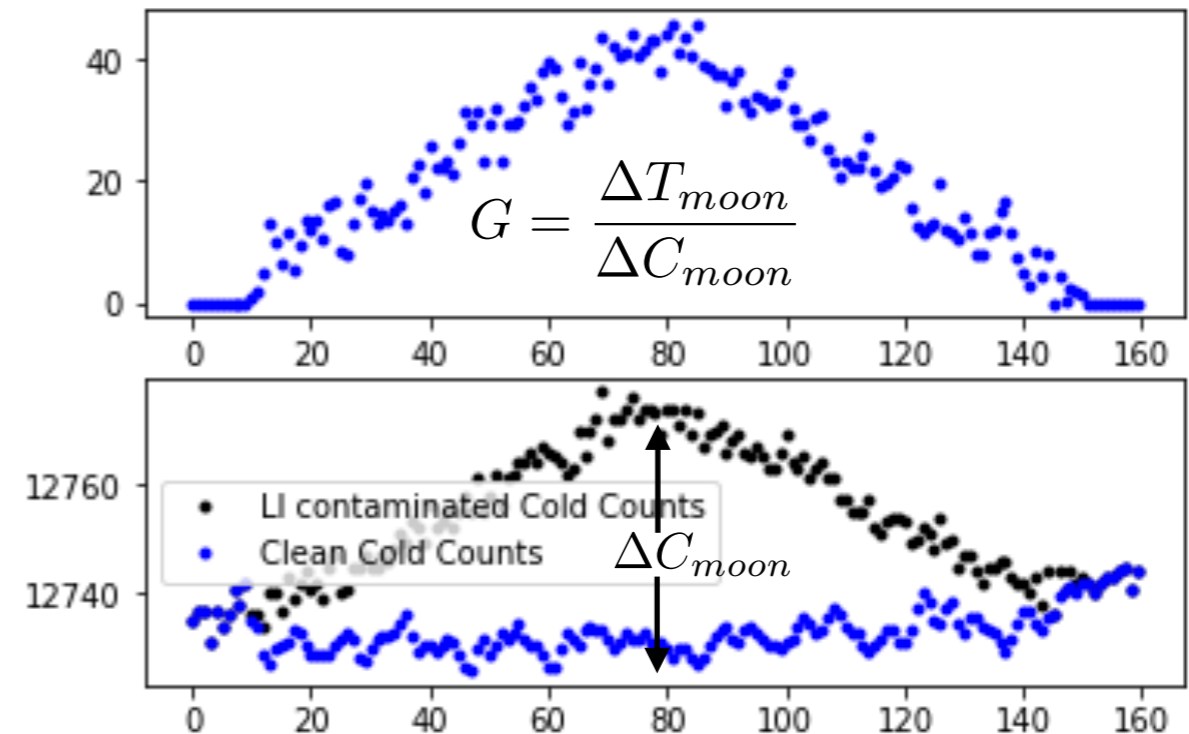
Potential of Taking Lunar Radiation as Cold End Calibration Reference for Instrument Across the Different Satellite Platform

- Radiance used in cold end is not clean cosmic background radiation, it includes contributions from other radiation sources such as Earth radiation from antenna sidelobe, thermal emission from reflector itself, as well as the thermal emission/reflection of satellite platform. The uncertainty of cold end radiance is different for each instrument and satellite platform, and is considered to be the major error source in TDR calibration.
- Lunar radiation is stable and highly predictable, and the lunar counts depends only on lunar radiance and instrument calibration gain. Therefore if a high accurate lunar radiance model can be established, the cold calibration radiance can be accurately determined by taking lunar radiance as reference.
- An absolute reference in cold end can not only improve the calibration accuracy, but also can reduce the inconsistency across the different satellite platform and therefore benefit for the development of CDR products

Sketch Plot of TDR Calibration

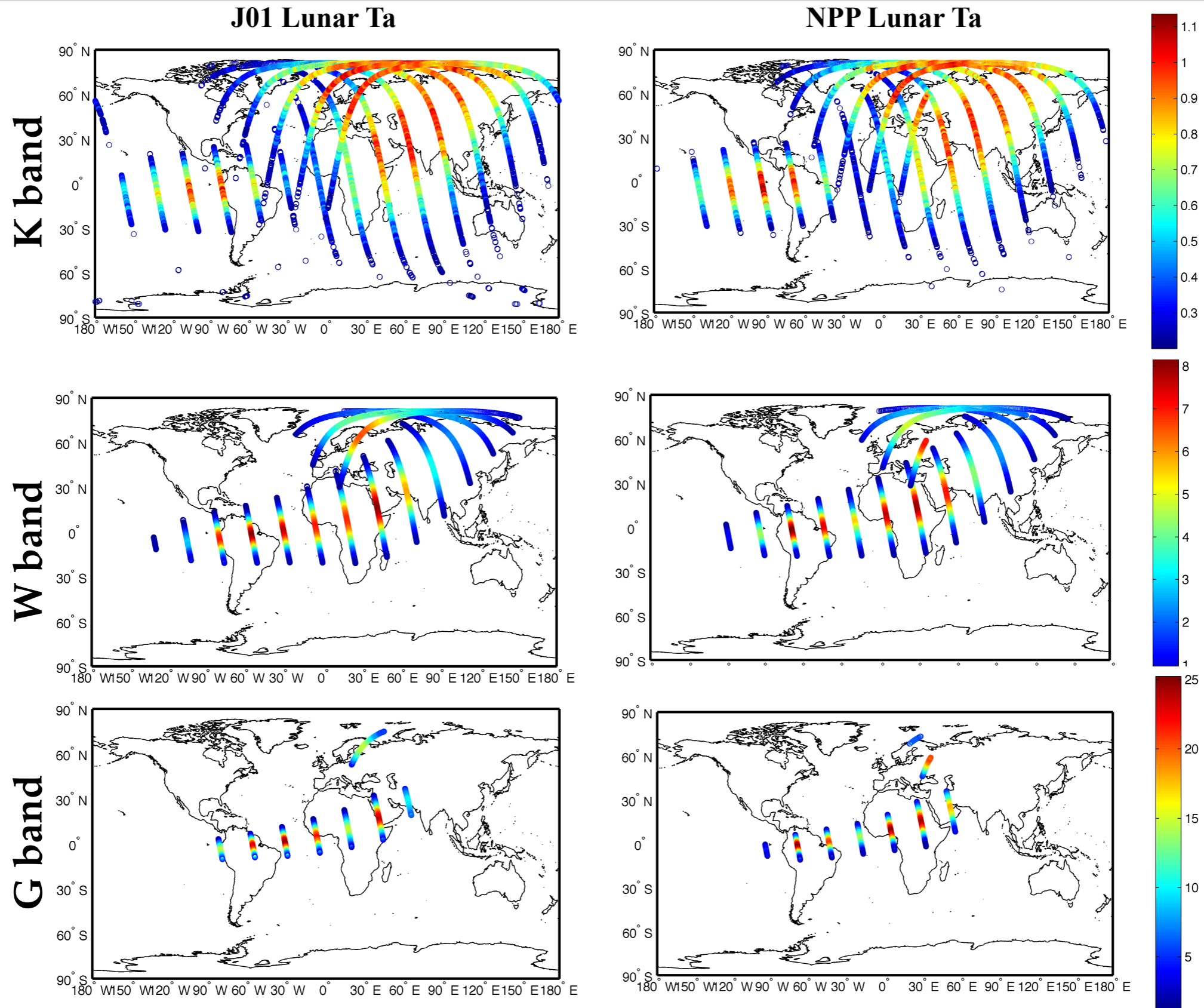


Lunar Calibration



Vicarious Calibration by Taking Moon as Reference

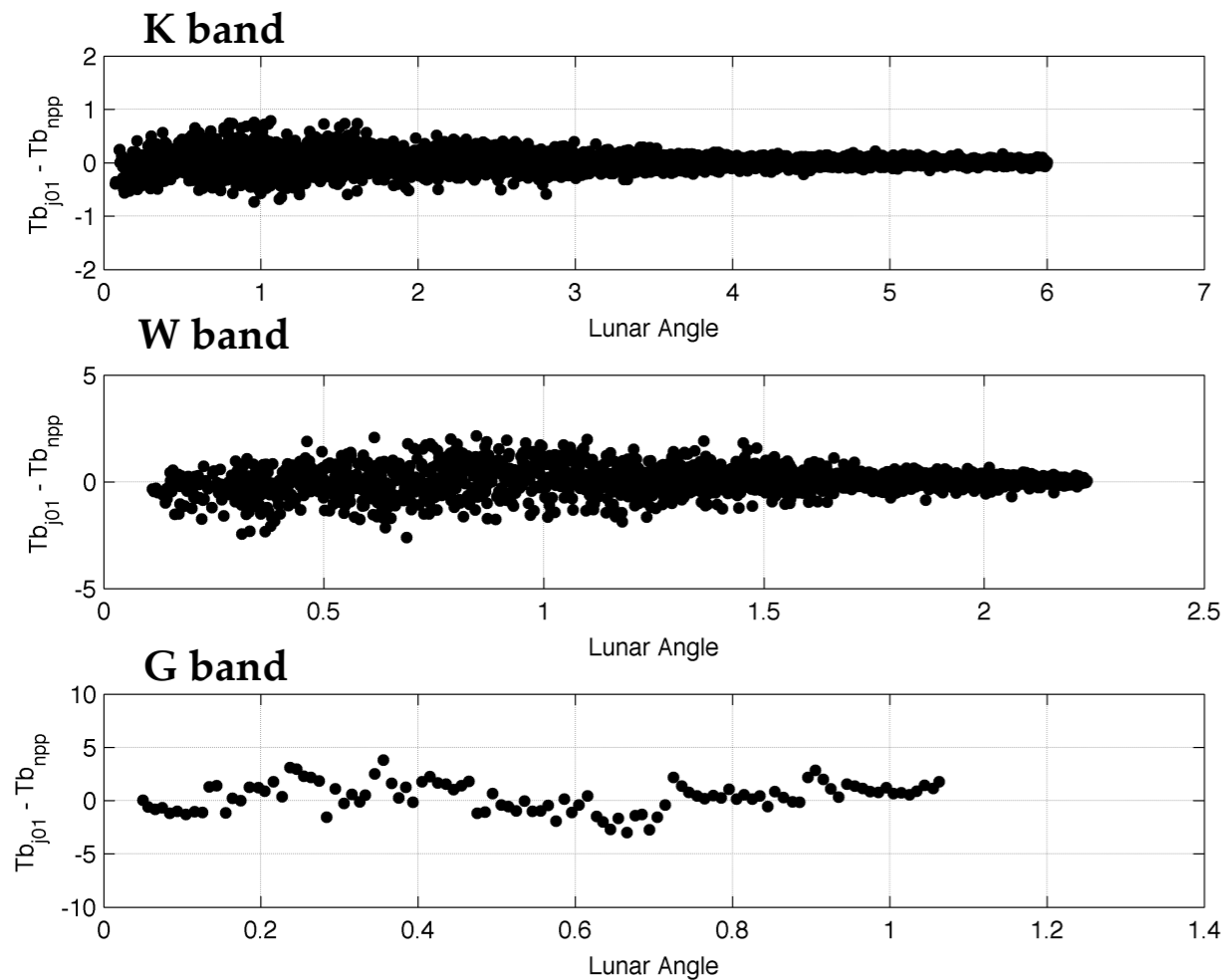
Hu Yang, Jun Zhou, Ninghai Sun, Kent Anderson, Quanhua Liu, Ed Kim, 2018, "Developing vicarious calibration for microwave sounding instruments using lunar radiation", *IEEE Transactions on Geoscience and Remote Sensing*, Vol.99, PP.1-11



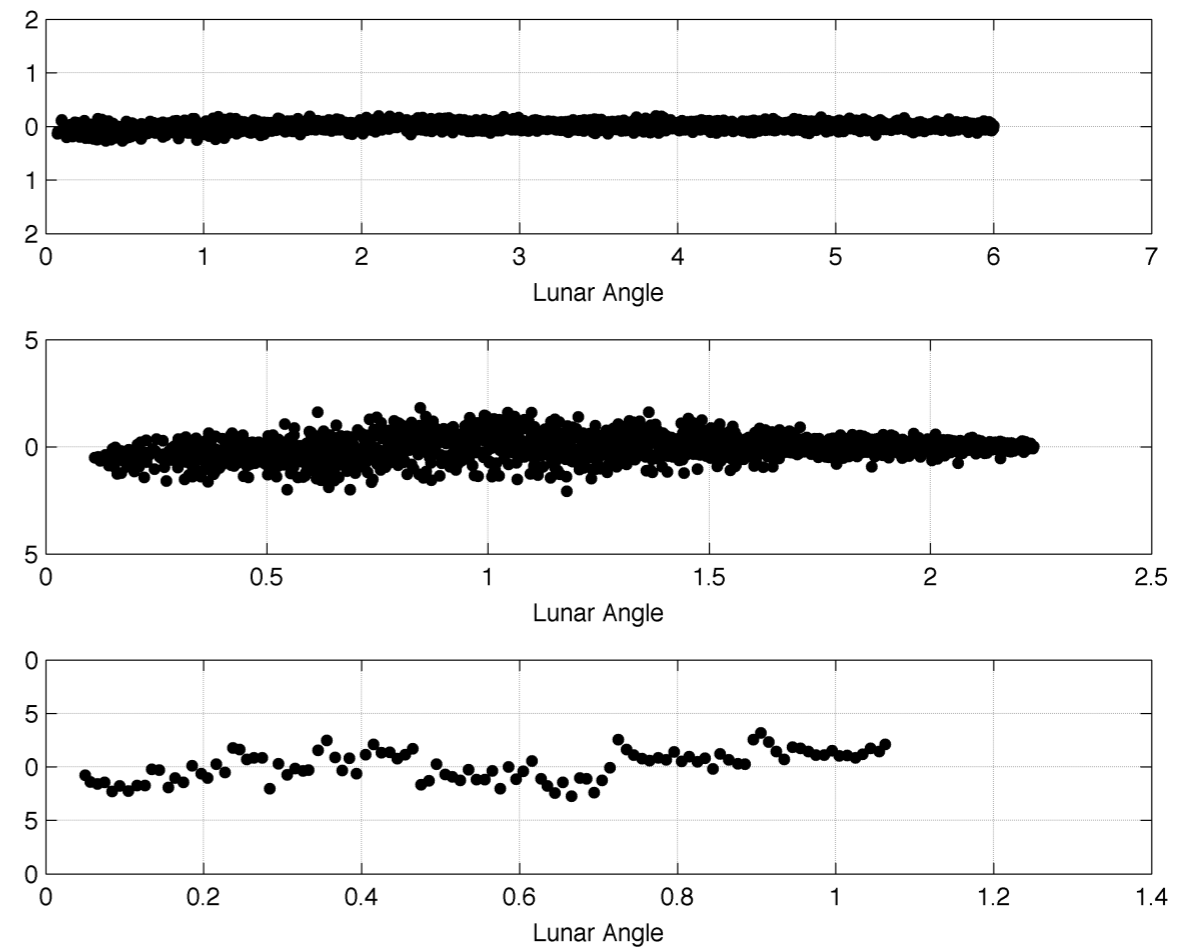
Inter-satellite Calibration between J01 and NPP

- Calibrated lunar Ta can be used to identify calibration difference between J01 and SNPP ATMS instruments
- Calibrated lunar Ta is very sensitive to pointing error at the angle near the antenna beam center
- Lunar model can be used to reduce impact of different pointing angle error in J01 and NPP

Ta(J01) - Ta (NPP)



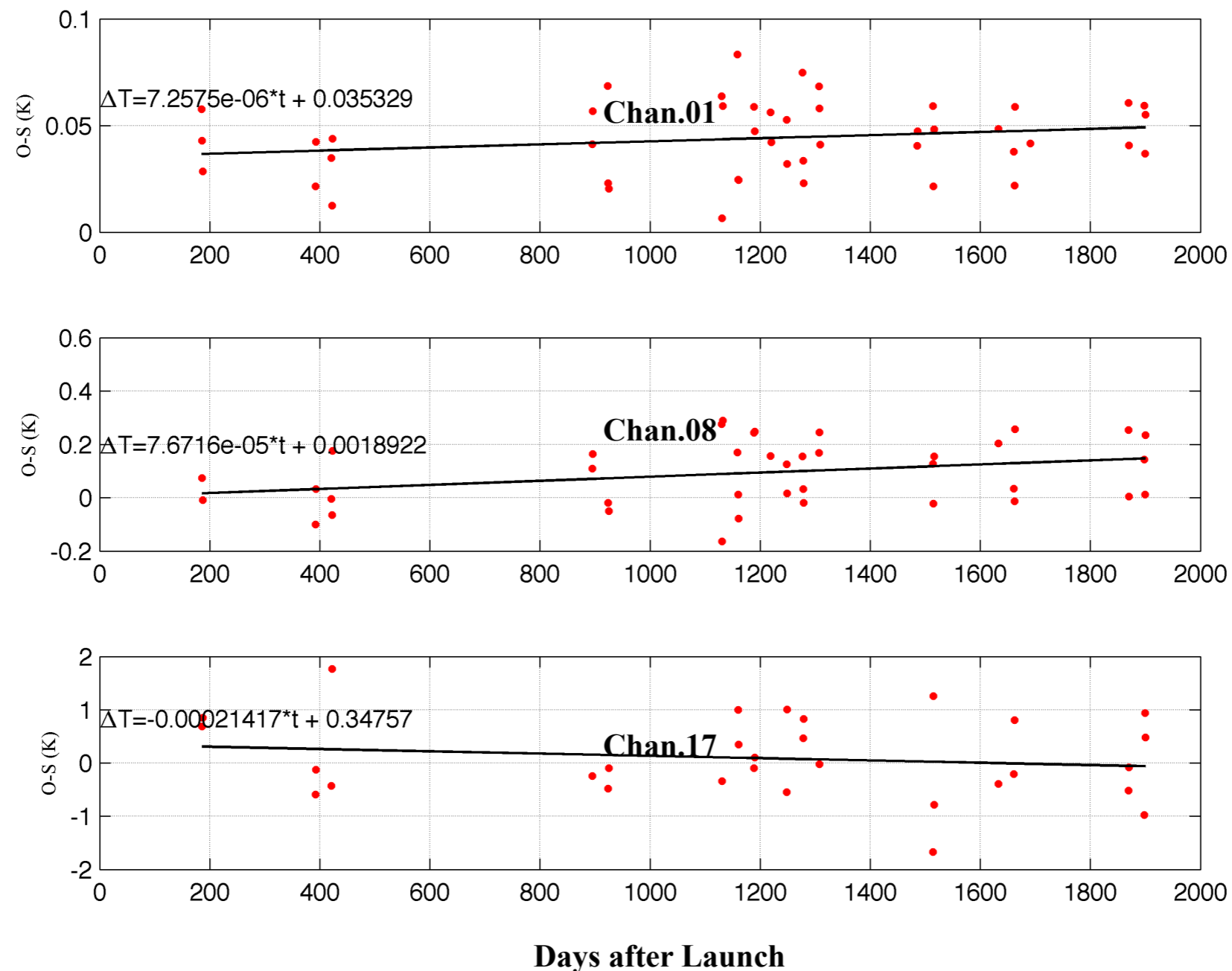
Lunar Model Corrected Ta Difference



Long-term Instrument Stability Monitoring

Lunar as a Permanent Reference Target can also help to evaluate the long-term calibration stability of microwave sensors. Here, the lunar brightness temperature model developed in this work is used to simulate the effective brightness temperature of moon's disk, and then compared with the measurements from ATMS instrument. Sensor calibration stability can then be evaluated as

$$S = d(\Delta T_{\text{moon}}^{\square})/dt$$



Conclusions and Future Work

- Lunar radiation is highly stable in microwave band and can be taken as permanent calibration reference target for microwave radiometers
- 2-D lunar scan observations from NOAA-20 ATMS and the lunar observations from drifting NOAA-18 AMSU provide a unique opportunity to obtain knowledge of lunar microwave brightness spectrum and phase lag in different frequency
- Future work is to build up a more comprehensive microwave emission model for Moon's surface based on knowledge gained from the satellite observations.